East Asian Journal on Applied Mathematics
doi: 10.4208/eajam.2024-041.220824

Vol. **16**, No. 1, pp. 45-71
February 2026

Energy Stable Splitting Schemes for Maxwell's Equations in Lorentz Media

Puttha Sakkaplangkul*

Department of Mathematics, School of Science, King Mongkut's Institute of Technology Ladkrabang, Bangkok 10520, Thailand.

Received 13 March 2024; Accepted (in revised version) 22 August 2024.

Abstract. In this paper, we introduce energy-stable schemes based on operator splitting methods for Maxwell's equations in two-dimensional Lorentz dispersive media with transverse electric polarization, namely the sequential splitting scheme (SS-ML) and the Strang-Marchuk splitting scheme (SM-ML). Each splitting scheme involves two substages per time step, where 1D discrete sub-problems are solved using the Crank-Nicolson method for time discretization. Both schemes ensure energy decay and unconditional stability. The convergence analysis reveals that the SS-ML scheme exhibits first-order accuracy in time and second-order accuracy in space based on the energy technique, while the SM-ML scheme achieves second-order accuracy in both time and space. Additionally, numerical dispersion analysis yields two discrete numerical dispersion relation identities for each scheme. Theoretical results are supported by examples and numerical experiments.

AMS subject classifications: 65N06, 65N12, 65N15, 65M06, 65M12

Key words: Maxwell equation, Lorentz model, finite difference, stability, Yee scheme.

1. Introduction

The study of wave propagation in dispersive media has gained considerable attention, particularly in light of the advancements in electromagnetic meta-materials. A dispersive medium is a substance or material that exhibits dispersion, a phenomenon where different wavelengths of light or electromagnetic radiation traverse the material at varying speeds. One particular type of dispersive material that demonstrates distinct frequency-dependent behavior in response to electromagnetic fields is a Lorentz medium. In a Lorentz material, modifications are made to Maxwell's equations accounting for the specific characteristics of the material's permittivity and permeability as described by the Lorentz model. The utility of Lorentz media extends across diverse domains, encompassing optics, solid-state physics, and materials research [3, 23, 27].

*Corresponding author. *Email address:* puttha.sa@kmitl.ac.th (P. Sakkaplangkul)

The Yee finite-difference time-domain (Yee-FDTD) method is a widely used technique for solving Maxwell's equations in the time domain [28, 29]. It discretizes the electric and magnetic fields on structured staggered space-time grids, enabling efficient simulations of electromagnetic wave propagation and interactions with various structures and materials. With its second-order accuracy in both space and time, the Yee-FDTD method is particularly suitable for electromagnetics, optics, and antenna design applications, delivering reliable and efficient solutions. Moreover, the Yee-FDTD method has been extended to handle Maxwell's equations in linear and nonlinear materials by combining it with other discrete methods [4, 5, 10, 28, 30]. The Yee-FDTD scheme has made significant extensions, particularly by accommodating nonuniform meshes within diverse material compositions [11, 20–22]. However, it exhibits a fundamental limitation as a conditionally stable numerical method. This conditionality dictates that both the time step and spatial step sizes must satisfy the Courant-Friedrichs-Lewy (CFL) stability condition during time-marching simulations [28]. Consequently, when spatial step sizes are reduced, the necessity for exceedingly minute time steps arises. This inherent demand for minuscule time steps places a significant computational burden on the conditionally stable Yee-FDTD method, particularly when addressing Maxwell's equations within extremely thin geometric structures [24].

To address the stability limitations and reduce computational expenses, the operator splitting method has been extensively studied for solving Maxwell's equations and is a widely adopted strategy for tackling complex time-dependent problems [7, 11, 13, 18]. This method involves breaking down complex time-dependent problems into simpler sub-problems, each focusing on a distinct physical process guided by a specific operator. These sub-problems are solved sequentially, and their solutions are combined using their initial conditions to solve the original problem. Commonly used operator splitting methods for time-dependent problems include sequential splitting, Strang-Marchuk splitting, and the alternating direction implicit (ADI-FDTD) approach. These methodology not only enhances computational efficiency compared with fully implicit techniques such as the Crank-Nicolson scheme but also maintain the critical attribute of unconditional stability. While the FDTD method is a powerful and widely used numerical technique in computational electromagnetics, it may not always preserve the energy conservation property, essential for ensuring physically meaningful simulations of electromagnetic phenomena. Chen *et al.* recently introduced energy-conserving splitting techniques for solving two- and three-dimensional Maxwell's equations [8, 9]. Additionally, extensions of the energy-based operator splitting method for Maxwell's equations in higher dimensions or with different materials have been proposed [2, 12, 14, 16, 25, 26].

In this paper, we introduce an operator splitting technique to solve the two-dimensional transverse electric Maxwell equations in Lorentz dispersive media. We formulate energy stable splitting methods based on the staggered Yee-grid structure, employing both sequential and Strang-Marchuk splitting schemes. These strategies entail two stages per time step, effectively reducing computational efforts. We present a rigorous analysis of the methods concerning stability and convergence of fully discrete splitting schemes using energy methods. Our analysis verifies that both splitting schemes satisfy the energy decay relation,

ensuring stable behavior in the discrete norm without imposing CFL restrictions [2, 26]. The absence of a CFL constraint is crucial when dealing with the complex Maxwell-Lorentz problem. As a result, similar to the Crank-Nicolson scheme, our techniques permit time step selection purely based on accuracy considerations. Unlike the Crank-Nicolson scheme, however, the sub-problem of diverse physical processes and dimensional splitting enhances computational efficiency. Furthermore, we establish that the Strang-Marchuk scheme achieves second-order accuracy in both time and space, whereas the sequential splitting scheme exhibits first-order accuracy in time and second-order accuracy in space. We also performed a numerical experiment to investigate the phase error, propagation angles, and angular frequencies of all schemes, as they play a crucial role in accurately predicting the behavior of electromagnetic waves and designing diverse electromagnetic systems. We validate the effectiveness of our splitting methods by comparing their numerical dispersion relations to exact dispersion relations. Additionally, we provide numerical examples in physical optics demonstrating characteristic phase error behavior across frequency ranges, highlighting the superior performance of our schemes compared to the Yee-FDTD approach. The theoretical results for the splitting schemes are further supported by corresponding numerical experiments.

The structure of this paper is as follows. In Section 2, we introduce the two-dimensional Maxwell's equations in Lorentz dispersive media and the energy decay results for this model. In Section 3, we present two fully discrete splitting schemes: the sequential scheme and Strang-Marchuk splitting scheme. The stability and convergence analyses of the fully discrete operator splitting schemes are presented in Sections 4 and 5, respectively. Additionally, we analyze the numerical dispersion of our schemes in Section 6. Numerical simulations to validate the theoretical results are provided in Section 7. Finally, the paper concludes in Section 8.

2. Models

Maxwell's equations are fundamental in electromagnetism, governing the behavior of the electric and magnetic fields and their interaction with electric charges and currents. Over a spatial domain denoted as Ω and a time interval within $[0, T]$, the Maxwell's equations in the absence of sources are expressed over the space-time region $\Omega\times[0, T]$ as follows:

$$\begin{aligned}
&\frac{\partial \mathbf{B}}{\partial t} = -\mathbf{curl}\ \mathbf{E},\\
&\frac{\partial \mathbf{D}}{\partial t} = \mathbf{curl}\ \mathbf{H},\\
&\nabla\cdot\mathbf{D} = 0,\\
&\nabla\cdot\mathbf{B} = 0,
\end{aligned} \tag{2.1}$$

where $\mathbf{E}$ is an electric field, $\mathbf{H}$ the magnetic field, $\mathbf{D}$ the electric flux density, and $\mathbf{B}$ the magnetic flux density. In dispersive dielectric materials with negligible magnetic effects, where there are no magnetic monopoles and magnetic sources, the electric displacement

field **D** and the magnetic field **B** still satisfy constitutive relations — viz.

$$\mathbf{B} = \mu_0 \mathbf{H}, \quad \mathbf{D} = \epsilon_0 \epsilon_\infty \mathbf{E} + \mathbf{P},$$

where ϵ_0 is the electric permittivity of free space, μ_0 is the magnetic permeability of free space, ϵ_∞ is the permittivity at infinite frequency, and **P** is the electric polarization field. The single-pole Lorentz model is a simplified representation of the dielectric response of a material to an electromagnetic field. It describes the time evolution of the polarization field **P** through the following equation [15, 30]:

$$\frac{\partial^2 \mathbf{P}}{\partial t^2} + \frac{1}{\tau}\frac{\partial \mathbf{P}}{\partial t} + \omega_0^2 \mathbf{P} = \epsilon_0 \omega_p^2 \mathbf{E},$$

where ω_0 is the resonance frequency of the medium, ω_p is the plasma frequency and $1/\tau$ is a damping constant. We assume that all parameters ω_0, ω_p, τ are constants within the medium.

By introducing the polarization density $\mathbf{J} = \partial \mathbf{P}/\partial t$, the Maxwell's equations (2.1) and the constitutive relations can be combined to yield the 3D-Maxwell-Lorentz model as follows:

$$\begin{aligned}
\frac{\partial \mathbf{H}}{\partial t} &= -\frac{1}{\mu_0}\mathbf{curl}\ \mathbf{E}, \\
\frac{\partial \mathbf{E}}{\partial t} &= \frac{1}{\epsilon_0 \epsilon_\infty}\mathbf{curl}\ \mathbf{H} - \frac{\mathbf{J}}{\epsilon_0 \epsilon_\infty}, \\
\frac{\partial \mathbf{J}}{\partial t} &= \epsilon_0 \omega_p^2 \mathbf{E} - \omega_0^2 \mathbf{P} - \frac{1}{\tau}\mathbf{J}, \\
\frac{\partial \mathbf{P}}{\partial t} &= \mathbf{J}.
\end{aligned} \tag{2.2}$$

In this paper, we examine the two-dimensional case of transverse electric (TE) polarization. The 2D scalar equations for TE polarization in the Maxwell-Lorentz framework can be derived from the Eq. (2.2) as

$$\frac{\partial H}{\partial t} = \frac{1}{\mu_0}\left(\frac{\partial E_x}{\partial y} - \frac{\partial E_y}{\partial x}\right), \tag{2.3}$$

$$\frac{\partial E_x}{\partial t} = \frac{1}{\epsilon_0 \epsilon_\infty}\frac{\partial H}{\partial y} - \frac{J_x}{\epsilon_0 \epsilon_\infty}, \tag{2.4}$$

$$\frac{\partial E_y}{\partial t} = -\frac{1}{\epsilon_0 \epsilon_\infty}\frac{\partial H}{\partial x} - \frac{J_y}{\epsilon_0 \epsilon_\infty}, \tag{2.5}$$

$$\frac{\partial J_x}{\partial t} = \epsilon_0 \omega_p^2 E_x - \omega_0^2 P_x - \frac{1}{\tau}J_x, \tag{2.6}$$

$$\frac{\partial J_y}{\partial t} = \epsilon_0 \omega_p^2 E_y - \omega_0^2 P_y - \frac{1}{\tau}J_y, \tag{2.7}$$

$$\frac{\partial P_x}{\partial t} = J_x, \tag{2.8}$$

$$\frac{\partial P_y}{\partial t} = J_y. \tag{2.9}$$

The system (2.3)-(2.9) is equipped with the perfect electric boundary condition (PEC) on the boundary of the rectangular domain $\Omega = [0,a]\times[0,b]$

$$E_x(x,0,t) = E_x(x,b,t) = E_y(0,y,t) = E_y(a,y,t) = 0 \quad \text{on } \partial\Omega\times(0,T],$$

along with initial conditions

$$H(\mathbf{x},0) = H_0(\mathbf{x}), \quad \mathbf{E}(\mathbf{x},0) = \mathbf{E}_0(\mathbf{x}), \quad \mathbf{J}(\mathbf{x},0) = \mathbf{J}_0(\mathbf{x}), \quad \mathbf{P}(\mathbf{x},0) = \mathbf{P}_0(\mathbf{x}), \quad \mathbf{x}\in\Omega.$$

To demonstrate that the Maxwell-Lorentz system (2.3)-(2.9) is well-posed, we construct a weak formulation. We first define two function spaces — viz.

$$H(\text{curl},\Omega) = \left\{\mathbf{u}\in\left(L^2(\Omega)\right)^2 \;\middle|\; \text{curl }\mathbf{u}\in L^2(\Omega)\right\},$$
$$H_0(\text{curl},\Omega) = \left\{\mathbf{u}\in H(\text{curl},\Omega) \;\middle|\; \mathbf{n}\times\mathbf{u} = \mathbf{0} \text{ on } \partial\Omega\right\},$$

where $\mathbf{n}$ is the outward unit normal vector to $\partial\Omega$ and $\text{curl}\,\mathbf{U} = \partial U_y/\partial x - \partial U_x/\partial y$ is the scalar curl operator for a vector field $\mathbf{U} = (U_x,U_y)^T$. We obtain the weak formulation for (2.3)-(2.9)

$$\left(\mu_0\frac{\partial H}{\partial t},v\right) = -(\text{curl }\mathbf{E},v) \qquad \text{for all } v\in L^2(\Omega),$$
$$\left(\epsilon_0\epsilon_\infty\frac{\partial \mathbf{E}}{\partial t},\mathbf{u}\right) = (H,\text{curl }\mathbf{u}) - (\mathbf{J},\mathbf{u}) \qquad \text{for all } \mathbf{u}\in H_0(\text{curl},\Omega),$$
$$\left(\frac{1}{\epsilon_0\omega_p^2}\frac{\partial \mathbf{J}}{\partial t},\mathbf{w}\right) = -\left(\frac{1}{\epsilon_0\omega_p^2\tau}\mathbf{J},\mathbf{w}\right) - \left(\frac{1}{\epsilon_0\epsilon_\infty(\epsilon_q-1)}\mathbf{P},\mathbf{w}\right) + (\mathbf{E},\mathbf{w}) \quad \text{for all } \mathbf{w}\in\left(L^2(\Omega)\right)^2,$$
$$\left(\frac{1}{\epsilon_0\epsilon_\infty(\epsilon_q-1)}\frac{\partial \mathbf{P}}{\partial t},\mathbf{q}\right) = \left(\frac{1}{\epsilon_0\epsilon_\infty(\epsilon_q-1)}\mathbf{J},\mathbf{q}\right) \qquad \text{for all } \mathbf{q}\in\left(L^2(\Omega)\right)^2,$$

where $(\cdot,\cdot)$ denotes the L^2 inner product. We use the notation $C^m(0,T;X)$ to represent the space of functions that are m times continuously differentiable from $[0,T]$ into the functional space X. In [17, 19, 26], the Maxwell-Lorentz model exhibits energy decay, as stated in the theorem below.

Theorem 2.1. *Let $\Omega\subset\mathscr{R}^2$ and suppose that $\mathbf{E} := (E_x,E_y)\in C(0,T:H_0(curl,\Omega))\cap C^1(0,T;(L^2(\Omega))^2), \mathbf{P} := (P_x,P_y), \mathbf{J} := (J_x,J_y)\in C^1(0,T;(L^2(\Omega))^2)$ and $H\in C^1(0,T;L^2(\Omega))$ are solutions of the weak formulation for the Maxwell-Lorentz system* (2.3)-(2.9) *along with the PEC boundary conditions. Then the system exhibits energy decay*

$$\mathscr{E}_L(t)\le\mathscr{E}_L(0) \quad \textit{for all} \quad t\ge 0,$$

where the energy function is defined as

$$\mathscr{E}_L(t) := \left[\mu_0\|H(t)\|_2^2 + \epsilon_0\epsilon_\infty\|\mathbf{E}(t)\|_2^2 + \frac{\omega_0^2}{\epsilon_0\omega_p^2}\|\mathbf{P}(t)\|_2^2 + \frac{1}{\epsilon_0\omega_p^2}\|\mathbf{J}(t)\|_2^2\right]^{1/2}.$$

Proof. See [19]. □

3. Splitting Schemes

In this section, we construct a splitting scheme by extending the ideas from [8, 25], which respectively applied sequential splitting to dimensional Maxwell's equations in a lossless medium with no source terms and Maxwell's equations in a Debye medium. This scheme is based on decomposing the curl operator into one-dimensional sub-problems as follows:

Stage 1.

$$\begin{aligned} \frac{\partial H}{\partial t} &= \frac{1}{\mu_0}\frac{\partial E_x}{\partial y}, \\ \frac{\partial E_x}{\partial t} &= \frac{1}{\epsilon_0\epsilon_\infty}\frac{\partial H}{\partial y}. \end{aligned} \tag{3.1}$$

Stage 2.

$$\begin{aligned} \frac{\partial H}{\partial t} &= -\frac{1}{\mu_0}\frac{\partial E_y}{\partial x}, \\ \frac{\partial E_x}{\partial t} &= -\frac{J_x}{\epsilon_0\epsilon_\infty}, \\ \frac{\partial E_y}{\partial t} &= -\frac{1}{\epsilon_0\epsilon_\infty}\frac{\partial H}{\partial x} - \frac{J_y}{\epsilon_0\epsilon_\infty}, \\ \frac{\partial J_x}{\partial t} &= \epsilon_0\omega_p^2 E_x - \omega_0^2 P_x - \frac{1}{\tau}J_x, \\ \frac{\partial J_y}{\partial t} &= \epsilon_0\omega_p^2 E_y - \omega_0^2 P_y - \frac{1}{\tau}J_y, \\ \frac{\partial P_x}{\partial t} &= J_x, \\ \frac{\partial P_y}{\partial t} &= J_y. \end{aligned} \tag{3.2}$$

We consider the systems (3.1) and (3.2) over the space-time domain $\Omega \times [0, T]$, where $\Omega = [0, a] \times [0, b]$ with $a, b, T > 0$, and apply the PEC boundary conditions.

3.1. Spatial and temporal discretization

In this paper, we focus on a space-time domain $\Omega \times [0, T]$, where Ω is defined as $[0, a] \times [0, b]$, with positive values for a, b, and T. We use $\triangle x$ and $\triangle y$ to denote the spatial step sizes, while $\triangle t$ represents the time step size. The discrete coordinates in both space and time are denoted as $(x_\alpha, y_\beta, t^\gamma)$, where $x_\alpha = \alpha\triangle x$, $y_\beta = \beta\triangle y$, and $t^\gamma = \gamma\triangle t$. We establish the definitions of discrete grid functions as follows:

$$U^\gamma_{\alpha,\beta} := U(x_\alpha, y_\beta, t^\gamma),$$

where U represents one of the components of the electromagnetic field, which can be any of the following: $H, E_x, E_y, J_x, J_y, P_x$ or P_y. The Degrees of Freedom (DoF) illustrated in

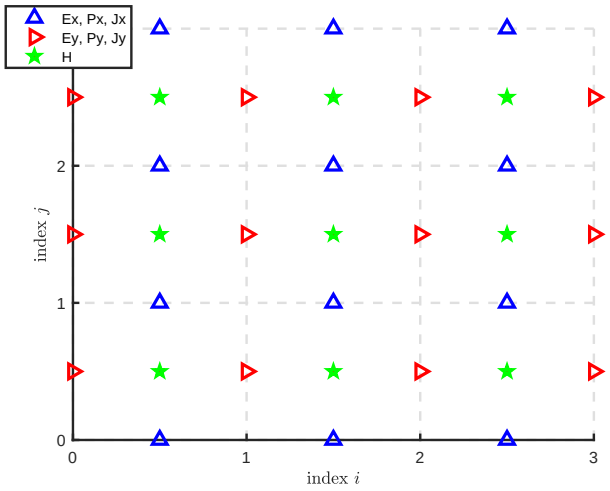

Figure 1: Staggered grids of electromagnetic fields.

Fig. 1 for the electric field components $E_\kappa, J_\kappa, P_\kappa$ on the staggered grid are located at the midpoint of the grid cell edge aligned with the κ-axis. In contrast, H_κ is positioned at the midpoint of the grid cell face that runs parallel to the κ-axis. This implies that, depending on the particular electromagnetic field in question, α can assume values of either i or $i+1/2$, β can be either j or $j+1/2$, and γ can take on values of either n or $n+1/2$.

Next, we establish standard definitions for centered spatial and temporal difference operators, along with the discrete time averaging operator as follows:

$$\delta_x U^\gamma_{\alpha,\beta} := \frac{U^\gamma_{\alpha+1/2,\beta} - U^\gamma_{\alpha-1/2,\beta}}{\triangle x}, \quad \delta_t U^\gamma_{\alpha,\beta} := \frac{U^{\gamma+1/2}_{\alpha,\beta} - U^{\gamma-1/2}_{\alpha,\beta}}{\triangle t},$$
$$\delta_y U^\gamma_{\alpha,\beta} := \frac{U^\gamma_{\alpha,\beta+1/2} - U^\gamma_{\alpha,\beta-1/2}}{\triangle y}, \quad \overline{U^\gamma_{\alpha,\beta}} := \frac{U^{\gamma+1/2}_{\alpha,\beta} + U^{\gamma-1/2}_{\alpha,\beta}}{2}.$$

3.2. Sequential splitting scheme

The SS-ML scheme, a sequential splitting scheme based on the 2D Maxwell-Lorentz TE equations, operates in two stages. It is applied to the discrete time interval $[t^n, t^{n+1}]$ with $0 \le n \le N-1$ as follows:

Stage 1. Compute intermediate variables $\widetilde{H}, \widetilde{E}_x$ from H^n, E^n_x on $[t^n, t^{n+1}]$

$$\frac{\widetilde{H}_{i+1/2,j+1/2} - H^n_{i+1/2,j+1/2}}{\Delta t} = \frac{1}{2\mu_0}\delta_y\Big(\widetilde{E}_{x_{i+1/2,j+1/2}} + E^n_{x_{i+1/2,j+1/2}}\Big), \tag{3.3}$$

$$\frac{\widetilde{E}_{x_{i+1/2,j}} - E^n_{x_{i+1/2,j}}}{\Delta t} = \frac{1}{2\epsilon_0\epsilon_\infty}\delta_y\Big(\widetilde{H}_{i+1/2,j} + H^n_{i+1/2,j}\Big). \tag{3.4}$$

Stage 2. Compute $H^{n+1}, E_x^{n+1}, E_y^{n+1}, J_x^{n+1}, J_y^{n+1}, P_x^{n+1}, P_y^{n+1}$ from intermediate variables $\widetilde{H}$, $\widetilde{E}_x$, E_y^n, J_x^n, J_y^n, P_x^n, P_y^n on $[t^n, t^{n+1}]$

$$\frac{H_{i+1/2,j+1/2}^{n+1} - \widetilde{H}_{i+1/2,j+1/2}}{\Delta t} = -\frac{1}{2\mu_0}\delta_x\Big(E_{y_{i+1/2,j+1/2}}^{n+1} + E_{y_{i+1/2,j+1/2}}^{n}\Big), \tag{3.5}$$

$$\frac{E_{x_{i+1/2,j}}^{n+1} - \widetilde{E}_{x_{i+1/2,j}}}{\Delta t} = -\frac{1}{\epsilon_0\epsilon_\infty}\overline{J_{x_{i+1/2,j}}^{n+1/2}}, \tag{3.6}$$

$$\frac{E_{y_{i,j+1/2}}^{n+1} - E_{y_{i,j+1/2}}^{n}}{\Delta t} = -\frac{1}{2\epsilon_0\epsilon_\infty}\delta_x\Big(H_{i,j+1/2}^{n+1} + \widetilde{H}_{i,j+1/2}\Big) - \frac{1}{\epsilon_0\epsilon_\infty}\overline{J_{y_{i,j+1/2}}^{n+1/2}}, \tag{3.7}$$

$$\frac{J_{x_{i+1/2,j}}^{n+1} - J_{x_{i+1/2,j}}^{n}}{\Delta t} = \frac{\epsilon_0}{2}\omega_p^2\Big(E_{x_{i+1/2,j}}^{n+1} + \widetilde{E}_{x_{i+1/2,j}}\Big) - \omega_0^2\overline{P_{x_{i+1/2,j}}^{n+1/2}} - \frac{1}{\tau}\overline{J_{x_{i+1/2,j}}^{n+1/2}}, \tag{3.8}$$

$$\frac{J_{y_{i,j+1/2}}^{n+1} - J_{y_{i,j+1/2}}^{n}}{\Delta t} = \epsilon_0\omega_p^2\overline{E_{y_{i,j+1/2}}^{n+1/2}} - \omega_0^2\overline{P_{y_{i,j+1/2}}^{n+1/2}} - \frac{1}{\tau}\overline{J_{y_{i,j+1/2}}^{n+1/2}}, \tag{3.9}$$

$$\frac{P_{x_{i+1/2,j}}^{n+1} - P_{x_{i+1/2,j}}^{n}}{\Delta t} = \overline{J_{x_{i+1/2,j}}^{n+1/2}}, \tag{3.10}$$

$$\frac{P_{y_{i,j+1/2}}^{n+1} - P_{y_{i,j+1/2}}^{n}}{\Delta t} = \overline{J_{y_{i,j+1/2}}^{n+1/2}}. \tag{3.11}$$

To achieve second-order in time accuracy, we enhanced the SS-ML scheme by introducing a three-stage process. This modification improves the scheme from first-order to second-order.

3.3. Strang-Marchuk splitting scheme

The SM-ML scheme, a Strang-Marchuk splitting scheme based on the 2D Maxwell-Lorentz TE equations, operates in three stages. It is applied to the discrete time interval $[t^n, t^{n+1}]$ with $0 \le n \le N-1$ as follows:

Stage 1. Compute intermediate variables $\widetilde{H}, \widetilde{E}_x$ from H^n, E_x^n on $[t^n, t^{n+1/2}]$

$$\frac{\widetilde{H}_{i+1/2,j+1/2} - H_{i+1/2,j+1/2}^{n}}{\Delta t} = \frac{1}{4\mu_0}\delta_y\Big(\widetilde{E}_{x_{i+1/2,j+1/2}} + E_{x_{i+1/2,j+1/2}}^{n}\Big),$$

$$\frac{\widetilde{E}_{x_{i+1/2,j}} - E_{x_{i+1/2,j}}^{n}}{\Delta t} = \frac{1}{4\epsilon_0\epsilon_\infty}\delta_y\Big(\widetilde{H}_{i+1/2,j} + H_{i+1/2,j}^{n}\Big).$$

Stage 2. Compute $\widehat{H}, \widehat{E}_x, E_y^{n+1}, J_x^{n+1}, J_y^{n+1}, P_x^{n+1}, P_y^{n+1}$ from variables $\widetilde{H}$, $\widetilde{E}_x$, E_y^n, J_x^n, J_y^n, P_x^n, P_y^n on $[t^n, t^{n+1}]$

$$\frac{\widehat{H}_{i+1/2,j+1/2} - \widetilde{H}_{i+1/2,j+1/2}}{\Delta t} = -\frac{1}{2\mu_0}\delta_x\Big(E_{y_{i+1/2,j+1/2}}^{n+1} + E_{y_{i+1/2,j+1/2}}^{n}\Big),$$

$$\frac{\widehat{E}_{x_{i+1/2,j}}-\widetilde{E}_{x_{i+1/2,j}}}{\Delta t}=-\frac{1}{\epsilon_0\epsilon_\infty}\overline{J^{n+1/2}_{x_{i+1/2,j}}},$$
$$\frac{E^{n+1}_{y_{i,j+1/2}}-E^{n}_{y_{i,j+1/2}}}{\Delta t}=-\frac{1}{2\epsilon_0\epsilon_\infty}\delta_x\Big(\widehat{H}_{i,j+1/2}+\widetilde{H}_{i,j+1/2}\Big)-\frac{1}{\epsilon_0\epsilon_\infty}\overline{J^{n+1/2}_{y_{i,j+1/2}}},$$
$$\frac{J^{n+1}_{x_{i+1/2,j}}-J^{n}_{x_{i+1/2,j}}}{\Delta t}=\frac{\epsilon_0}{2}\omega_p^2\Big(\widehat{E}_{x_{i+1/2,j}}+\widetilde{E}_{x_{i+1/2,j}}\Big)-\omega_0^2\overline{P^{n+1/2}_{x_{i+1/2,j}}}-\frac{1}{\tau}\overline{J^{n+1/2}_{x_{i+1/2,j}}},$$
$$\frac{J^{n+1}_{y_{i,j+1/2}}-J^{n}_{y_{i,j+1/2}}}{\Delta t}=\epsilon_0\omega_p^2\overline{E^{n+1/2}_{y_{i,j+1/2}}}-\omega_0^2\overline{P^{n+1/2}_{y_{i,j+1/2}}}-\frac{1}{\tau}\overline{J^{n+1/2}_{y_{i,j+1/2}}},$$
$$\frac{P^{n+1}_{x_{i+1/2,j}}-P^{n}_{x_{i+1/2,j}}}{\Delta t}=\overline{J^{n+1/2}_{x_{i+1/2,j}}},$$
$$\frac{P^{n+1}_{y_{i,j+1/2}}-P^{n}_{y_{i,j+1/2}}}{\Delta t}=\overline{J^{n+1/2}_{y_{i,j+1/2}}}.$$

Stage 3. Compute H^{n+1}, E_x^{n+1} from $\widehat{H}, \widehat{E}_x$ on $[t^{n+1/2}, t^{n+1}]$

$$\frac{H^{n+1}_{i+1/2,j+1/2}-\widehat{H}_{i+1/2,j+1/2}}{\Delta t}=\frac{1}{4\mu_0}\delta_y\Big(E^{n+1}_{x_{i+1/2,j+1/2}}+\widehat{E}_{x_{i+1/2,j+1/2}}\Big),$$
$$\frac{E^{n+1}_{x_{i+1/2,j}}-\widehat{E}_{x_{i+1/2,j}}}{\Delta t}=\frac{1}{4\epsilon_0\epsilon_\infty}\delta_y\Big(H^{n+1}_{i+1/2,j}+\widehat{H}_{i+1/2,j}\Big).$$

We apply the perfect electric conductor (PEC) boundary conditions to both the SS-ML scheme and the SM-ML scheme, which can be represented in scalar forms as follows: For $0\le i\le I-1$ and $0\le j\le J-1$,

$$E^n_{x_{i+1/2,0}}=E^n_{x_{i+1/2,J}}=E^n_{y_{0,j+1/2}}=E^n_{y_{I,j+1/2}}=0. \tag{3.12}$$

4. Stability and Energy Analysis

In this section, our aim is to assess the stability of the operator splitting schemes and demonstrate their energy decay properties, similar to their continuous counterparts. To achieve this, we establish both a discrete inner product and a discrete L^2 norm for the electromagnetic field.

Let

$$W:=\big\{W_{i+1/2,j+1/2}\big\},\quad \mathbf{F}:=\big\{\big(U_{i+1/2,j},V_{i,j+1/2}\big)\big\},$$
$$\widetilde{W}:=\big\{\widetilde{W}_{i+1/2,j+1/2}\big\},\quad \widetilde{\mathbf{F}}:=\big\{\big(\widetilde{U}_{i+1/2,j},\widetilde{V}_{i,j+1/2}\big)\big\}$$

represent sets of discrete meshes containing grid functions of electromagnetic fields. We define the discrete inner products of these two fields as follows:

$$\langle U,\widetilde{U}\rangle_{E_x}=\Delta_h\sum_{i=0}^{I-1}\sum_{j=0}^{J-1}U_{i+1/2,j}\widetilde{U}_{i+1/2,j},$$

$$\langle W, \widetilde{W} \rangle_H = \Delta_h \sum_{i=0}^{I-1} \sum_{j=0}^{J-1} W_{i+1/2,j+1/2} \widetilde{W}_{i+1/2,j+1/2},$$
$$\langle V, \widetilde{V} \rangle_{E_y} = \Delta_h \sum_{i=0}^{I-1} \sum_{j=0}^{J-1} V_{i,j+1/2} \widetilde{V}_{i,j+1/2},$$

where $\Delta_h = \Delta x \Delta y$. The corresponding discrete L^2 grid norms are defined by

$$\|U\|_{E_x}^2 = \Delta_h \sum_{i=0}^{I-1} \sum_{j=0}^{J-1} |U_{i+1/2,j}|^2, \qquad \|V\|_{E_y}^2 = \Delta_h \sum_{i=0}^{I-1} \sum_{j=0}^{J-1} |V_{i,j+1/2}|^2,$$
$$\|W\|_H^2 = \Delta_h \sum_{i=0}^{I-1} \sum_{j=0}^{J-1} |W_{i+1/2,j+1/2}|^2, \quad \|\mathbf{F}\|_E^2 = \|U\|_{E_x}^2 + \|V\|_{E_y}^2.$$

We initially introduce a summation by parts property necessary for proving the stability of our schemes, as stated in the following lemma.

Lemma 4.1 (cf. Refs. [6,8]). *Let U, V, W be the discrete grid functions defined on the discrete meshes. Suppose that U and V satisfy the PEC boundary conditions*

$$U_{i+1/2,0} = U_{i+1/2,J} = V_{0,j+1/2} = V_{I,j+1/2},$$

where $0 \le i \le I-1$ and $0 \le j \le J-1$. For any integers $0 < i < I-1$ and $0 < j < J-1$, we have

$$\sum_{i=0}^{I-1} W_{i+1/2,j+1/2} \delta_x V_{i+1/2,j+1/2} = -\sum_{i=1}^{I-1} V_{i,j+1/2} \delta_x W_{i,j+1/2},$$
$$\sum_{j=0}^{J-1} W_{i+1/2,j+1/2} \delta_y U_{i+1/2,j+1/2} = -\sum_{j=1}^{J-1} U_{i+1/2,j} \delta_y W_{i+1/2,j}.$$

Based on this lemma, the following theorems demonstrate the preservation of energy decay characteristics in our schemes within the continuous problem.

4.1. Energy decay property and unconditional stability

Theorem 4.1 (Energy Decay Property for SS-ML Scheme). *For the integer $n \ge 0$, let*

$$H^n := \left\{ H_{i+1/2,j+1/2}^n \right\}, \qquad \mathbf{E}^n := \left\{ \left(E_{x_{i+1/2,j}}^n, E_{y_{i,j+1/2}}^n \right) \right\},$$
$$\mathbf{J}^n := \left\{ \left(J_{x_{i+1/2,j}}^n, J_{y_{i,j+1/2}}^n \right) \right\}, \quad \mathbf{P}^n := \left\{ \left(P_{x_{i+1/2,j}}^n, P_{y_{i,j+1/2}}^n \right) \right\}$$

be the solutions of SS-ML scheme, then the SS-ML scheme with the PEC boundary conditions (3.12) *satisfies the discrete energy decay*

$$\mathscr{E}_L^{n+1} \le \mathscr{E}_L^n, \tag{4.1}$$

where the discrete energy is defined as

$$\mathscr{E}_L^n := \left[\mu_0 \|H^n\|_H^2 + \epsilon_0\epsilon_\infty \|\mathbf{E}^n\|_E^2 + \frac{\omega_0^2}{\epsilon_0\omega_p^2}\|\mathbf{P}^n\|_E^2 + \frac{1}{\epsilon_0\omega_p^2}\|\mathbf{J}^n\|_E^2 \right]^{1/2}. \tag{4.2}$$

Proof. Multiplying the Eq. (3.3) with $\mu_0\Delta t\Delta_h\,(\widetilde{H}_{i+1/2,j+1/2}+H^n_{i+1/2,j+1/2})$, the Eq. (3.4) with $\epsilon_0\epsilon_\infty\Delta t\Delta_h(\widetilde{E}_{x_{i+1/2,j}}+E^n_{x_{i+1/2},j})$, and summing over all spatial nodes, we obtain

$$\begin{aligned}
&\mu_0\|\widetilde{H}\|_H^2 + \epsilon_0\epsilon_\infty\|\widetilde{E}_x\|_{E_x}^2 \\
&= \mu_0\|H^n\|_H^2 + \epsilon_0\epsilon_\infty\|E_x^n\|_{E_x}^2 + \frac{\Delta t}{2}\left\langle \widetilde{H}+H^n, \delta_y\left(\widetilde{E}_x+E_x^n\right)\right\rangle_H \\
&\quad + \frac{\Delta t}{2}\left\langle \widetilde{E}_x+E_x^n, \delta_y\left(\widetilde{H}+H^n\right)\right\rangle_{E_x}.
\end{aligned} \tag{4.3}$$

Similarly, multiplying the Eq. (3.5) by $\mu_0\Delta t\Delta_h(H^{n+1}_{i+1/2,j+1/2}+\widetilde{H}_{i+1/2,j+1/2})$, the Eq. (3.6) by $\epsilon_0\epsilon_\infty\Delta t\Delta_h(E^{n+1}_{x_{i+1/2,j}}+\widetilde{E}_{x_{i+1/2,j}})$, the Eq. (3.7) by $\epsilon_0\epsilon_\infty\Delta t\Delta_h(E^{n+1}_{y_{i,j+1/2}}+E^n_{y_{i,j+1/2}})$, the Eq. (3.8) by $\Delta t\Delta_h(J^{n+1}_{x_{i+1/2,j}}+J^n_{x_{i+1/2,j}})/(\epsilon_0\omega_p^2)$, the Eq. (3.9) by $\Delta t\Delta_h(J^{n+1}_{y_{i,j+1/2}}+J^n_{y_{i,j+1/2}})/(\epsilon_0\omega_p^2)$, the Eq. (3.10) by $\omega_0^2\Delta t\Delta_h(P^{n+1}_{x_{i+1/2,j}}+P^n_{x_{i+1/2,j}})/(\epsilon_0\omega_p^2)$, the Eq. (3.11) by $\omega_0^2\Delta t\Delta_h\,(P^{n+1}_{y_{i,j+1/2}}+P^n_{y_{i,j+1/2}})/(\epsilon_0\omega_p^2)$ and summing over all spatial nodes, we obtain

$$\begin{aligned}
&\mu_0\|H^{n+1}\|_H^2 + \epsilon_0\epsilon_\infty\|\mathbf{E}^{n+1}\|_E^2 + \frac{1}{\epsilon_0\omega_p^2}\|\mathbf{J}^{n+1}\|_E^2 + \frac{\omega_0^2}{\epsilon_0\omega_p^2}\|\mathbf{P}^{n+1}\|_E^2 \\
&= \mu_0\|\widetilde{H}\|_H^2 + \epsilon_0\epsilon_\infty\left(\|\widetilde{E}_x\|_{E_x}^2 + \|E_y^n\|_{E_y}^2\right) + \frac{\|\mathbf{J}^n\|_E^2}{\epsilon_0\omega_p^2} + \frac{\omega_0^2}{\epsilon_0\omega_p^2}\|\mathbf{P}^n\|_E^2 \\
&\quad - \frac{\Delta t}{2}\left\langle H^{n+1}+\widetilde{H}, \delta_x\left(E_y^{n+1}+E_y^n\right)\right\rangle_H - \frac{\Delta t}{2}\left\langle E_y^{n+1}+E_y^n, \delta_x\left(H^{n+1}+\widetilde{H}\right)\right\rangle_{E_y} \\
&\quad - \frac{\Delta t}{2\tau}\frac{1}{\epsilon_0\omega_p^2}\left\|J_x^{n+1}+J_x^n\right\|_{E_x}^2 - \frac{\Delta t}{2\tau}\frac{1}{\epsilon_0\omega_p^2}\left\|J_y^{n+1}+J_y^n\right\|_{E_y}^2.
\end{aligned} \tag{4.4}$$

By Lemma 4.1, combining Eqs. (4.3) and (4.4) and using the fact that the discrete norm is non-negative, the discrete energy (4.2) satisfies the energy decay (4.1). □

The following theorem asserts that the SM-ML scheme conserves an equivalent discrete energy decay property as the SS-ML system.

Theorem 4.2 (Energy Decay Property for SM-ML Scheme)**.** *For the integer $n \geq 0$, let*

$$\begin{aligned}
H^n &:= \left\{H^n_{i+1/2,j+1/2}\right\}, \qquad \mathbf{E}^n := \left\{\left(E^n_{x_{i+1/2,j}}, E^n_{y_{i,j+1/2}}\right)\right\}, \\
\mathbf{J}^n &:= \left\{\left(J^n_{x_{i+1/2,j}}, J^n_{y_{i,j+1/2}}\right)\right\}, \quad \mathbf{P}^n := \left\{\left(P^n_{x_{i+1/2,j}}, P^n_{y_{i,j+1/2}}\right)\right\}
\end{aligned}$$

be the solutions of SM-ML scheme, then the SM-ML scheme with the PEC boundary conditions (3.12) *satisfies the discrete energy decay*

$$\mathscr{E}_L^{n+1} \leq \mathscr{E}_L^n,$$

where the discrete energy is defined in (4.2).

5. Convergence Analysis

In this section, we establish the convergence of energy-based operator splitting techniques. To assess the truncation errors, we initially introduce intermediate variables as follows:

$$\widetilde{H}^*(\mathbf{z},t^n)=H(\mathbf{z},t^n)+\frac{\Delta t^2}{8\mu_0\epsilon_0\epsilon_\infty}\delta_{yy}H(\mathbf{z},t^n)+\frac{\Delta t}{2\mu_0}\delta_y E_x(\mathbf{z},t^n), \tag{5.1}$$

$$\widetilde{E}_x^*(\mathbf{z},t^n)=E_x(\mathbf{z},t^n)+\frac{\Delta t^2}{8\mu_0\epsilon_0\epsilon_\infty}\delta_{yy}E_x(\mathbf{z},t^n)+\frac{\Delta t}{2\epsilon_0\epsilon_\infty}\delta_y H(\mathbf{z},t^n), \tag{5.2}$$

$$\widehat{H}^*(\mathbf{z},t^{n+1})=H(\mathbf{z},t^{n+1})+\frac{\Delta t^2}{8\mu_0\epsilon_0\epsilon_\infty}\delta_{yy}H(\mathbf{z},t^{n+1})-\frac{\Delta t}{2\mu_0}\delta_y E_x(\mathbf{z},t^{n+1}), \tag{5.3}$$

$$\widehat{E}_x^*(\mathbf{z},t^{n+1})=E_x(\mathbf{z},t^{n+1})+\frac{\Delta t^2}{8\mu_0\epsilon_0\epsilon_\infty}\delta_{yy}E_x(\mathbf{z},t^{n+1})-\frac{\Delta t}{2\epsilon_0\epsilon_\infty}\delta_y H(\mathbf{z},t^{n+1}), \tag{5.4}$$

where $\mathbf{z}=(x,y)$ denotes a point in space. We set

$$\overline{W(\mathbf{z},t^{n+1/2})}=\frac{1}{2}\big(W(\mathbf{z},t^{n+1})+W(\mathbf{z},t^n)\big)$$

and let discrete point notations

$$\mathbf{z}^k_{\alpha/2,\beta}=(x_{\alpha+1/2},y_\beta,t^k),\quad \mathbf{z}^k_{\alpha,\beta/2}=(x_\alpha,y_{\beta+1/2},t^k),\quad \mathbf{z}^n_{\alpha/2,\beta/2}=(x_{\alpha+1/2},y_{\beta+1/2},t^k).$$

The local error functions obtained by the intermediate variables, (5.1)-(5.4), and the exact solutions in the SM-ML scheme are defined by

Stage 1.

$$\begin{aligned}
\xi_{11_{i+1/2,j+1/2}}&=\frac{\widetilde{H}^*\big(\mathbf{z}^n_{i/2,j/2}\big)-H\big(\mathbf{z}^n_{i/2,j/2}\big)}{\Delta t}-\frac{1}{4\mu_0}\delta_y\Big(\widetilde{E}_x^*\big(\mathbf{z}^n_{i/2,j/2}\big)+E_x\big(\mathbf{z}^n_{i/2,j/2}\big)\Big),\\
\xi_{12_{i+1/2,j}}&=\frac{\widetilde{E}_x^*\big(\mathbf{z}^n_{i/2,j}\big)-E_x\big(\mathbf{z}^n_{i/2,j}\big)}{\Delta t}-\frac{1}{4\epsilon_0\epsilon_\infty}\delta_y\Big(\widetilde{H}^*\big(\mathbf{z}^n_{i/2,j}\big)+H\big(\mathbf{z}^n_{i/2,j}\big)\Big).
\end{aligned} \tag{5.5}$$

Stage 2.

$$\xi_{21_{i+1/2,j+1/2}}=\frac{\widehat{H}^*\big(\mathbf{z}^{n+1}_{i/2,j/2}\big)-\widetilde{H}^*\big(\mathbf{z}^n_{i/2,j/2}\big)}{\Delta t}+\frac{1}{2\mu_0}\delta_x\Big(E_y\big(\mathbf{z}^{n+1}_{i/2,j/2}\big)+E_y\big(\mathbf{z}^n_{i/2,j/2}\big)\Big), \tag{5.6a}$$

$$\xi_{22_{i+1/2,j}}=\frac{\widehat{E}_x^*\big(\mathbf{z}^{n+1}_{i/2,j}\big)-\widetilde{E}_x^*\big(\mathbf{z}^n_{i/2,j}\big)}{\Delta t}+\frac{1}{\epsilon_0\epsilon_\infty}\overline{J_x\big(\mathbf{z}^{n+1/2}_{i/2,j}\big)}, \tag{5.6b}$$

$$\begin{aligned}
\xi_{23_{i,j+1/2}}&=\frac{E_y\big(\mathbf{z}^{n+1}_{i,j/2}\big)-E_y\big(\mathbf{z}^n_{i,j/2}\big)}{\Delta t}+\frac{1}{2\epsilon_0\epsilon_\infty}\delta_x\Big(\widehat{H}^*\big(\mathbf{z}^{n+1}_{i,j/2}\big)+\widetilde{H}^*\big(\mathbf{z}^n_{i,j/2}\big)\Big)\\
&\quad+\frac{1}{\epsilon_0\epsilon_\infty}\overline{J_y\big(\mathbf{z}^{n+1/2}_{i,j/2}\big)},
\end{aligned} \tag{5.6c}$$

$$\xi_{24_{i+1/2,j}} = \frac{J_x\big(\mathbf{z}^{n+1}_{i/2,j}\big)-J_x\big(\mathbf{z}^{n}_{i/2,j}\big)}{\Delta t} - \frac{\epsilon_0}{2}\omega_p^2\Big(\widehat{E}^*_x\big(\mathbf{z}^{n+1}_{i/2,j}\big)+\widetilde{E}^*_x\big(\mathbf{z}^{n}_{i/2,j}\big)\Big) + \omega_0^2\overline{P_x\big(\mathbf{z}^{n+1/2}_{i/2,j}\big)}+\frac{1}{\tau}\overline{J_x\big(\mathbf{z}^{n+1/2}_{i/2,j}\big)}, \tag{5.6d}$$

$$\xi_{25_{i,j+1/2}} = \frac{J_y\big(\mathbf{z}^{n+1}_{i,j/2}\big)-J_y\big(\mathbf{z}^{n}_{i,j/2}\big)}{\Delta t} - \epsilon_0\omega_p^2\overline{E_y\big(\mathbf{z}^{n+1/2}_{i,j/2}\big)} + \omega_0^2\overline{P_y\big(\mathbf{z}^{n+1/2}_{i,j/2}\big)}+\frac{1}{\tau}\overline{J_y\big(\mathbf{z}^{n+1/2}_{i,j/2}\big)}, \tag{5.6e}$$

$$\xi_{26_{i+1/2,j}} = \frac{P_x\big(\mathbf{z}^{n+1}_{i/2,j}\big)-P_x\big(\mathbf{z}^{n}_{i/2,j}\big)}{\Delta t} - \overline{J_x\big(\mathbf{z}^{n+1/2}_{i/2,j}\big)}, \tag{5.6f}$$

$$\xi_{27_{i,j+1/2}} = \frac{P_y\big(\mathbf{z}^{n+1}_{i,j/2}\big)-P_y\big(\mathbf{z}^{n}_{i,j/2}\big)}{\Delta t} - \overline{J_y\big(\mathbf{z}^{n+1/2}_{i,j/2}\big)}. \tag{5.6g}$$

Stage 3.

$$\begin{aligned}
\xi_{31_{i+1/2,j+1/2}} &= \frac{H\big(\mathbf{z}^{n+1}_{i/2,j/2}\big)-\widehat{H}^*\big(\mathbf{z}^{n+1}_{i/2,j/2}\big)}{\Delta t} - \frac{1}{4\mu_0}\delta_y\Big(E_x\big(\mathbf{z}^{n+1}_{i/2,j/2}\big)+\widehat{E}^*_x\big(\mathbf{z}^{n+1}_{i/2,j/2}\big)\Big),\\
\xi_{32_{i+1/2,j}} &= \frac{E_x\big(\mathbf{z}^{n+1}_{i/2,j}\big)-\widehat{E}^*_x\big(\mathbf{z}^{n+1}_{i/2,j}\big)}{\Delta t} - \frac{1}{4\epsilon_0\epsilon_\infty}\delta_y\Big(H\big(\mathbf{z}^{n+1}_{i/2,j}\big)+\widehat{H}^*\big(\mathbf{z}^{n+1}_{i/2,j}\big)\Big).
\end{aligned} \tag{5.7}$$

Proposition 5.1. *Suppose that the exact solutions of electromagnetic fields are smooth enough:* $\mathbf{E},\mathbf{P},\mathbf{J}\in C^3(0,T;[C^3(\overline{\Omega})]^2)$ *and* $H\in C^3(0,T;C^3(\overline{\Omega}))$. *Let* ξ_{1i},ξ_{2j} *and* ξ_{3k} *where* $i,k=1,2$ *and* $j=1,2,\dots,7$ *be local error functions of the SM-ML scheme defined as* (5.5)-(5.7). *Then for* $i,k=1,2$ *and* $j=1,2,\dots,7$, *there exists a positive constant* C_{sm} *independent of* $\Delta t,\Delta x$ *and* Δy *such that*

$$\max_n\big\{\|\xi_{1i}\|_{\ell_\infty},\|\xi_{2j}\|_{\ell_\infty},\|\xi_{3k}\|_{\ell_\infty}\big\}\le C_{sm}\big(\Delta t^2+\Delta x^2+\Delta y^2\big). \tag{5.8}$$

Proof. By performing the Taylor expansion around appropriate temporal points and applying the regularity condition of the exact solutions, the local error functions (5.5)-(5.7) are

$$\begin{aligned}
\xi_{11_{i+1/2,j+1/2}} &= -\frac{1}{32}\frac{\Delta t^2}{\mu_0^2\epsilon_0\epsilon_\infty}\delta_y^3E_x\big(\mathbf{z}^n_{i/2,j/2}\big),\\
\xi_{12_{i+1/2,j}} &= -\frac{1}{32}\frac{\Delta t^2}{\mu_0\epsilon_0^2\epsilon_\infty^2}\delta_y^3H\big(\mathbf{z}^n_{i/2,j}\big),\\
\xi_{21_{i+1/2,j+1/2}} &= \tau^a_{CN}+\frac{\Delta t^2}{8\mu_0\epsilon_0\epsilon_\infty}\delta_y^2\left[\partial_tH\big(\mathbf{z}^{n+1/2}_{i/2,j/2}\big)+\frac{\Delta t^2}{24}\partial_t^3H\big(\mathbf{z}^{n+1/2}_{i/2,j/2}\big)\right],\\
\xi_{22_{i+1/2,j}} &= \tau^b_{CN}+\frac{\Delta t^2}{8\mu_0\epsilon_0\epsilon_\infty}\delta_y^2\left[\partial_tE_x\big(\mathbf{z}^{n+1/2}_{i/2,j}\big)+\frac{\Delta t^2}{24}\partial_t^3E_x\big(\mathbf{z}^{n+1/2}_{i/2,j}\big)\right],
\end{aligned}$$

$$\xi_{23_{i,j+1/2}} = \tau^c_{CN} - \Delta t^2\left[\frac{1}{4\mu_0\epsilon_0\epsilon_\infty}\delta_x\delta_y\partial_t E_x\big(\mathbf{z}^{n+1/2}_{i,j/2}\big) - \frac{1}{8\mu_0\epsilon_0^2\epsilon_\infty^2}\delta_x\delta_y^2 H\big(\mathbf{z}^{n+1/2}_{i,j/2}\big)\right],$$

$$\xi_{24_{i+1/2,j}} = \tau^d_{CN} + \Delta t^2\left[\frac{1}{4\epsilon_0\epsilon_\infty}\epsilon_0\omega_p^2\delta_y\partial_t H\big(\mathbf{z}^{n+1/2}_{i/2,j}\big) - \frac{1}{8\mu_0\epsilon_\infty}\omega_p^2\delta_y^2 E_x\big(\mathbf{z}^{n+1/2}_{i/2,j}\big)\right],$$

$$\xi_{25_{i,j+1/2}} = \Delta t^2\Big[\frac{1}{24}\partial_t^3 J_y\big(\mathbf{z}^{n+1/2}_{i,j/2}\big) - \frac{\epsilon_0}{8}\omega_p^2\partial_t^2 E_y\big(\mathbf{z}^{n+1/2}_{i,j/2}\big) + \frac{\omega_0^2}{8}\partial_t^2 P_y\big(\mathbf{z}^{n+1/2}_{i,j/2}\big) + \frac{1}{8\tau}\partial_t^2 J_y\big(\mathbf{z}^{n+1/2}_{i,j/2}\big)\Big],$$

$$\xi_{26_{i+1/2,j}} = \Delta t^2\left[\frac{1}{24}\partial_t^3 P_x\big(\mathbf{z}^{n+1/2}_{i/2,j}\big) - \frac{1}{8}\partial_t^2 J_x\big(\mathbf{z}^{n+1/2}_{i/2,j}\big)\right],$$

$$\xi_{27_{i,j+1/2}} = \Delta t^2\left[\frac{1}{24}\partial_t^3 P_y\big(\mathbf{z}^{n+1/2}_{i,j/2}\big) - \frac{1}{8}\partial_t^2 J_y\big(\mathbf{z}^{n+1/2}_{i,j/2}\big)\right],$$

$$\xi_{31_{i+1/2,j+1/2}} = -\frac{1}{32}\frac{\Delta t^2}{\mu_0^2\epsilon_0\epsilon_\infty}\delta_y^3 E_x\big(\mathbf{z}^{n+1}_{i/2,j/2}\big),$$

$$\xi_{32_{i+1/2,j}} = -\frac{1}{32}\frac{\Delta t^2}{\mu_0\epsilon_0^2\epsilon_\infty^2}\delta_y^3 H\big(\mathbf{z}^{n+1}_{i/2,j/2}\big),$$

where $\tau^a_{CN}, \tau^b_{CN}, \tau^c_{CN}$ and τ^d_{CN} represent the local truncation errors of the Crank-Nicolson scheme for Eqs. (2.3) to (2.6), respectively. By performing the Taylor expansion around appropriate points in space and time, the local error functions (5.5)-(5.7) are shown to be second-order accurate in both space and time, so the identity (5.8) holds. □

Similarly, the local error functions obtained by the intermediate variables (5.1) and (5.2) for the SS-ML scheme can be presented by

Stage 1.

$$\begin{aligned}
\eta_{11_{i+1/2,j+1/2}} &= \frac{\widetilde{H}^*\big(\mathbf{z}^n_{i/2,j/2}\big) - H\big(\mathbf{z}^n_{i/2,j/2}\big)}{\Delta t} - \frac{1}{2\mu_0}\delta_y\Big(\widetilde{E}^*_x\big(\mathbf{z}^n_{i/2,j/2}\big) + E_x\big(\mathbf{z}^n_{i/2,j/2}\big)\Big),\\
\eta_{12_{i+1/2,j}} &= \frac{\widetilde{E}^*_x\big(\mathbf{z}^n_{i/2,j}\big) - E_x\big(\mathbf{z}^n_{i/2,j}\big)}{\Delta t} - \frac{1}{2\epsilon_0\epsilon_\infty}\delta_y\Big(\widetilde{H}^*\big(\mathbf{z}^n_{i/2,j}\big) + H\big(\mathbf{z}^n_{i/2,j}\big)\Big).
\end{aligned} \tag{5.9}$$

Stage 2.

$$\eta_{21_{i+1/2,j+1/2}} = \frac{H\big(\mathbf{z}^{n+1}_{i/2,j/2}\big) - \widetilde{H}^*\big(\mathbf{z}^n_{i/2,j/2}\big)}{\Delta t} + \frac{1}{2\mu_0}\delta_x\Big(E_y\big(\mathbf{z}^{n+1}_{i/2,j/2}\big) + E_y\big(\mathbf{z}^n_{i/2,j/2}\big)\Big), \tag{5.10a}$$

$$\eta_{22_{i+1/2,j}} = \frac{E_x\big(\mathbf{z}^{n+1}_{i/2,j}\big) - \widetilde{E}^*_x\big(\mathbf{z}^n_{i/2,j}\big)}{\Delta t} + \frac{1}{\epsilon_0\epsilon_\infty}\overline{J_x\big(\mathbf{z}^{n+1/2}_{i/2,j}\big)}, \tag{5.10b}$$

$$\eta_{23_{i,j+1/2}} = \frac{E_y\big(\mathbf{z}^{n+1}_{i,j/2}\big) - E_y\big(\mathbf{z}^n_{i,j/2}\big)}{\Delta t} + \frac{1}{2\epsilon_0\epsilon_\infty}\delta_x\Big(H\big(\mathbf{z}^{n+1}_{i,j/2}\big) + \widetilde{H}^*\big(\mathbf{z}^n_{i,j/2}\big)\Big)$$

$$+\frac{1}{\epsilon_0\epsilon_\infty}\overline{J_y\big(\mathbf{z}_{i,j/2}^{n+1/2}\big)}, \tag{5.10c}$$

$$\eta_{24_{i+1/2,j}}=\frac{J_x\big(\mathbf{z}_{i/2,j}^{n+1}\big)-J_x\big(\mathbf{z}_{i/2,j}^{n}\big)}{\Delta t}-\frac{\epsilon_0}{2}\omega_p^2\Big(E_x\big(\mathbf{z}_{i/2,j}^{n+1}\big)+\widetilde{E}_x^*\big(\mathbf{z}_{i/2,j}^{n}\big)\Big)+\omega_0^2\overline{P_x\big(\mathbf{z}_{i/2,j}^{n+1/2}\big)}$$
$$+\frac{1}{\tau}\overline{J_x\big(\mathbf{z}_{i/2,j}^{n+1/2}\big)}, \tag{5.10d}$$

$$\eta_{25_{i,j+1/2}}=\frac{J_y\big(\mathbf{z}_{i,j/2}^{n+1}\big)-J_y\big(\mathbf{z}_{i,j/2}^{n}\big)}{\Delta t}-\epsilon_0\omega_p^2\overline{E_y\big(\mathbf{z}_{i,j/2}^{n+1/2}\big)}+\omega_0^2\overline{P_y\big(\mathbf{z}_{i,j/2}^{n+1/2}\big)}$$
$$+\frac{1}{\tau}\overline{J_y\big(\mathbf{z}_{i,j/2}^{n+1/2}\big)}, \tag{5.10e}$$

$$\eta_{26_{i+1/2,j}}=\frac{P_x\big(\mathbf{z}_{i/2,j}^{n+1}\big)-P_x\big(\mathbf{z}_{i/2,j}^{n}\big)}{\Delta t}-\overline{J_x\big(\mathbf{z}_{i/2,j}^{n+1/2}\big)}, \tag{5.10f}$$

$$\eta_{27_{i,j+1/2}}=\frac{P_y\big(\mathbf{z}_{i,j/2}^{n+1}\big)-P_y\big(\mathbf{z}_{i,j/2}^{n}\big)}{\Delta t}-\overline{J_y\big(\mathbf{z}_{i,j/2}^{n+1/2}\big)}. \tag{5.10g}$$

By similar analysis, the local error function of the SS-ML scheme is of the first order in time perturbation as the following proposition.

Proposition 5.2. *Suppose that the exact solutions of electromagnetic fields are smooth enough:* $\mathbf{E},\mathbf{P},\mathbf{J}\in C^3(0,T;[C^3(\overline{\Omega})]^2)$ *and* $H\in C^3(0,T;C^3(\overline{\Omega}))$. *Let* η_{1i} *and* η_{2j} *where* $i=1,2$ *and* $j=1,2,\ldots,7$ *be local error functions of the SS-ML scheme defined as* (5.9) *and* (5.10). *Then for* $i=1,2$ *and* $j=1,2,\ldots,7$, *there exists a positive constant* C_{ss} *independent of* $\Delta t,\Delta x$ *and* Δy *such that*

$$\max_n\big\{\|\eta_{1i}\|_{\ell_\infty},\|\eta_{2j}\|_{\ell_\infty}\big\}\le C_{ss}\big(\Delta t+\Delta x^2+\Delta y^2\big).$$

Proof. The proof of this proposition is similar to the proof of Proposition 5.1. □

Next, we examine the convergence of the SM-ML scheme. We define the error functions on the staggered grids (x_α,y_β) at time t^n as follows:

$$\begin{aligned}
\mathscr{W}_{\kappa_{\alpha,\beta}}^n&=W_\kappa(x_\alpha,y_\beta,t^n)-W_{\kappa_{\alpha,\beta}}^n,\\
\widetilde{\widetilde{W}}_{\kappa_{\alpha,\beta}}&=\widetilde{W}_\kappa^*(x_\alpha,y_\beta,t^n)-\widetilde{W}_{\kappa_{\alpha,\beta}},\\
\widehat{\widehat{W}}_{\kappa_{\alpha,\beta}}&=\widehat{W}_\kappa^*(x_\alpha,y_\beta,t^n)-\widehat{W}_{\kappa_{\alpha,\beta}},
\end{aligned}\tag{5.11}$$

where $\kappa\in\{x,y\}$. The error functions at time t^n can be represented by the vector $\mathscr{W}^n=(\mathscr{W}_x^n,\mathscr{W}_y^n,\mathscr{W}_z^n)$. The convergence proof relies on the energy method and truncation analysis, as shown in the following theorem.

Theorem 5.1. *Suppose that the exact solutions of electromagnetic fields are smooth enough:* $\mathbf{E},\mathbf{P},\mathbf{J}\in C^3(0,T;[C^3(\overline{\Omega})]^2)$ *and* $H\in C^3(0,T;C^3(\overline{\Omega}))$. *For all* $n\ge 0$, *let* $\mathbf{E}^n,\mathbf{P}^n,\mathbf{J}^n$ *and* H^n *be the solutions of the SM-ML scheme. Then for fixed* $T=N\Delta t>0$, *there exists a constant* C *independent of* $\Delta t,\Delta x$ *and* Δy *such that*

$$\max_{0\le n\le N}\mathbf{Err}_h^n\le e^{4T}\max_{0\le n\le N}\mathbf{Err}_h^0+C(\Delta t^2+\Delta x^2+\Delta y^2)^2,$$

where

$$\mathbf{Err}_h^n := \mu_0\|H(t^n)-H^n\|_H^2+\epsilon_0\epsilon_\infty\|\mathbf{E}(t^n)-\mathbf{E}^n\|_E^2+\frac{\omega_0^2}{\epsilon_0\omega_p^2}\|\mathbf{P}(t^n)-\mathbf{P}^n\|_E^2+\frac{\|\mathbf{J}(t^n)-\mathbf{J}^n\|_E^2}{\epsilon_0\omega_p^2}.$$

Proof. The error function (5.11) on the staggered grids (x_α, y_β) at time t^n can be written similarly to SM-ML scheme as

Stage 1.

$$\begin{aligned}
&\frac{\widetilde{\widetilde{H}}_{i+1/2,j+1/2}-\mathscr{H}^n_{i+1/2,j+1/2}}{\Delta t}=\frac{1}{4\mu_0}\delta_y\Big(\widetilde{\widetilde{E}}_{x_{i+1/2,j+1/2}}+\mathscr{E}^n_{x_{i+1/2,j+1/2}}\Big)+\xi_{11_{i+1/2,j+1/2}},\\
&\frac{\widetilde{\widetilde{E}}_{x_{i+1/2,j}}-\mathscr{E}^n_{x_{i+1/2,j}}}{\Delta t}=\frac{1}{4\epsilon_0\epsilon_\infty}\delta_y\Big(\widetilde{\widetilde{H}}_{i+1/2,j}+\mathscr{H}^n_{i+1/2,j}\Big)+\xi_{12_{i+1/2,j}}.
\end{aligned}\tag{5.12}$$

Stage 2.

$$\begin{aligned}
&\frac{\widehat{\widehat{H}}_{i+1/2,j+1/2}-\widetilde{\widetilde{H}}_{i+1/2,j+1/2}}{\Delta t}=-\frac{1}{2\mu_0}\delta_x\Big(\mathscr{E}^{n+1}_{y_{i+1/2,j+1/2}}+\mathscr{E}^n_{y_{i+1/2,j+1/2}}\Big)+\xi_{21_{i+1/2,j+1/2}},\\
&\frac{\widehat{\widehat{E}}_{x_{i+1/2,j}}-\widetilde{\widetilde{E}}_{x_{i+1/2,j}}}{\Delta t}=-\frac{1}{\epsilon_0\epsilon_\infty}\overline{\mathscr{J}^{n+1/2}_{x_{i+1/2,j}}}+\xi_{22_{i+1/2,j}},\\
&\frac{\mathscr{E}^{n+1}_{y_{i,j+1/2}}-\mathscr{E}^n_{y_{i,j+1/2}}}{\Delta t}=-\frac{1}{2\epsilon_0\epsilon_\infty}\delta_x\Big(\widehat{\widehat{H}}_{i,j+1/2}+\widetilde{\widetilde{H}}_{i,j+1/2}\Big)-\frac{1}{\epsilon_0\epsilon_\infty}\overline{\mathscr{J}^{n+1/2}_{y_{i,j+1/2}}}+\xi_{23_{i,j+1/2}},\\
&\frac{\mathscr{J}^{n+1}_{x_{i+1/2,j}}-\mathscr{J}^n_{x_{i+1/2,j}}}{\Delta t}=\frac{\epsilon_0}{2}\omega_p^2\Big(\widehat{\widehat{E}}_{x_{i+1/2,j}}+\widetilde{\widetilde{E}}_{x_{i+1/2,j}}\Big)-\omega_0^2\overline{\mathscr{P}^{n+1/2}_{x_{i+1/2,j}}}-\frac{1}{\tau}\overline{\mathscr{J}^{n+1/2}_{x_{i+1/2,j}}}+\xi_{24_{i+1/2,j}},\\
&\frac{\mathscr{J}^{n+1}_{y_{i,j+1/2}}-\mathscr{J}^n_{y_{i,j+1/2}}}{\Delta t}=\epsilon_0\omega_p^2\overline{\mathscr{E}^{n+1/2}_{y_{i,j+1/2}}}-\omega_0^2\overline{\mathscr{P}^{n+1/2}_{y_{i,j+1/2}}}-\frac{1}{\tau}\overline{\mathscr{J}^{n+1/2}_{y_{i,j+1/2}}}+\xi_{25_{i,j+1/2}},\\
&\frac{\mathscr{P}^{n+1}_{x_{i+1/2,j}}-\mathscr{P}^n_{x_{i+1/2,j}}}{\Delta t}=\overline{\mathscr{J}^{n+1/2}_{x_{i+1/2,j}}}+\xi_{26_{i+1/2,j}},\\
&\frac{\mathscr{P}^{n+1}_{y_{i,j+1/2}}-\mathscr{P}^n_{y_{i,j+1/2}}}{\Delta t}=\overline{\mathscr{J}^{n+1/2}_{y_{i,j+1/2}}}+\xi_{27_{i,j+1/2}}.
\end{aligned}\tag{5.13}$$

Stage 3.

$$\begin{aligned}
&\frac{\mathscr{H}^{n+1}_{i+1/2,j+1/2}-\widehat{\widehat{H}}_{i+1/2,j+1/2}}{\Delta t}=\frac{1}{4\mu_0}\delta_y\Big(\mathscr{E}^{n+1}_{x_{i+1/2,j+1/2}}+\widehat{\widehat{E}}_{x_{i+1/2,j+1/2}}\Big)+\xi_{31_{i+1/2,j+1/2}},\\
&\frac{\mathscr{E}^{n+1}_{x_{i+1/2,j}}-\widehat{\widehat{E}}_{x_{i+1/2,j}}}{\Delta t}=\frac{1}{4\epsilon_0\epsilon_\infty}\delta_y\Big(\mathscr{H}^{n+1}_{i+1/2,j}+\widehat{\widehat{H}}_{i+1/2,j}\Big)+\xi_{32_{i+1/2,j}}.
\end{aligned}\tag{5.14}$$

Similar to the proof of Theorem 4.1, using the Eq. (5.12), we get

$$\begin{aligned}&\mu_0\Big(\|\widetilde{\widetilde{H}}\|_H^2-\|\mathscr{H}^n\|_H^2\Big)+\epsilon_0\epsilon_\infty\Big(\|\widetilde{\widetilde{E}}_x\|_{E_x}^2-\|\mathscr{E}_x^n\|_{E_x}^2\Big)\\&=\Delta t\mu_0\Big\langle\widetilde{\widetilde{H}}+\mathscr{H}^n,\xi_{11}\Big\rangle_H+\Delta t\epsilon_0\epsilon_\infty\Big\langle\widetilde{\widetilde{E}}+\mathscr{E}_x^n,\xi_{12}\Big\rangle_{E_x}.\end{aligned}\tag{5.15}$$

The Young's inequality and Proposition 5.1 yield the existence of a constant C_1 such that the inequality (5.15) becomes

$$\begin{aligned}&\left(1-\frac{\Delta t}{2}\right)\Big[\mu_0\|\widetilde{\widetilde{H}}\|_H^2+\epsilon_0\epsilon_\infty\|\widetilde{\widetilde{E}}_x\|_{E_x}^2\Big]\\&\le\left(1+\frac{\Delta t}{2}\right)\Big[\mu_0\|\mathscr{H}^n\|_H^2+\epsilon_0\epsilon_\infty\|\mathscr{E}_x^n\|_{E_x}^2\Big]\\&\quad+\Delta tC_1(\Delta t^2+\Delta x^2+\Delta y^2)^2.\end{aligned}\tag{5.16}$$

By similar process, from Eqs. (5.13) and (5.14), we get

$$\begin{aligned}&\left(1-\frac{\Delta t}{2}\right)\left[\mu_0\|\widehat{\widetilde{H}}\|_H^2+\epsilon_0\epsilon_\infty\|\widehat{\widetilde{E}}_x\|_{E_x}^2+\epsilon_0\epsilon_\infty\|\mathscr{E}_y^{n+1}\|_{E_y}^2+\frac{\omega_0^2}{\epsilon_0\omega_p^2}\|\mathscr{P}^{n+1}\|_E^2+\frac{\|\mathscr{J}^{n+1}\|_E^2}{\epsilon_0\omega_p^2}\right]\\&\le\left(1+\frac{\Delta t}{2}\right)\left[\mu_0\|\widetilde{\widetilde{H}}\|_H^2+\epsilon_0\epsilon_\infty\|\widetilde{\widetilde{E}}_x\|_{E_x}^2+\epsilon_0\epsilon_\infty\|\mathscr{E}_y^n\|_{E_y}^2+\frac{\omega_0^2}{\epsilon_0\omega_p^2}\|\mathscr{P}^n\|_E^2+\frac{\|\mathscr{J}^n\|_E^2}{\epsilon_0\omega_p^2}\right]\\&\quad+\Delta tC_2(\Delta t^2+\Delta x^2+\Delta y^2)^2,\end{aligned}\tag{5.17}$$

$$\begin{aligned}&\left(1-\frac{\Delta t}{2}\right)\Big[\mu_0\|\mathscr{H}^{n+1}\|_H^2+\epsilon_0\epsilon_\infty\|\mathscr{E}_x^{n+1}\|_{E_x}^2\Big]\\&\le\left(1+\frac{\Delta t}{2}\right)\Big[\mu_0\|\widehat{\widetilde{H}}\|_H^2+\epsilon_0\epsilon_\infty\|\widehat{\widetilde{E}}_x\|_{E_x}^2\Big]+\Delta tC_3(\Delta t^2+\Delta x^2+\Delta y^2)^2.\end{aligned}\tag{5.18}$$

Adding to both sides of (5.18) the term

$$E_1=\left(1-\frac{\Delta t}{2}\right)\left(\epsilon_0\epsilon_\infty\|\mathscr{E}_y^{n+1}\|_{E_y}^2+\frac{\omega_0^2}{\epsilon_0\omega_p^2}\|\mathscr{P}^{n+1}\|_E^2+\frac{\|\mathscr{J}^{n+1}\|_E^2}{\epsilon_0\omega_p^2}\right)$$

and dividing the result by $1+\Delta t/2$ gives

$$\begin{aligned}&\frac{(1-\Delta t/2)}{(1+\Delta t/2)}\left[\mu_0\|\mathscr{H}^{n+1}\|_H^2+\epsilon_0\epsilon_\infty\|\mathscr{E}^{n+1}\|_E^2+\frac{\omega_0^2}{\epsilon_0\omega_p^2}\|\mathscr{P}^{n+1}\|_E^2+\frac{\|\mathscr{J}^{n+1}\|_E^2}{\epsilon_0\omega_p^2}\right]\\&\le\left[\mu_0\|\widehat{\widetilde{H}}\|_H^2+\epsilon_0\epsilon_\infty\|\widehat{\widetilde{E}}_x\|_{E_x}^2+\epsilon_0\epsilon_\infty\|\mathscr{E}_y^{n+1}\|_{E_y}^2+\frac{\omega_0^2}{\epsilon_0\omega_p^2}\|\mathscr{P}^{n+1}\|_E^2+\frac{\|\mathscr{J}^{n+1}\|_E^2}{\epsilon_0\omega_p^2}\right]\\&\quad+\frac{2\Delta t}{2+\Delta t}C_3(\Delta t^2+\Delta x^2+\Delta y^2)^2.\end{aligned}\tag{5.19}$$

Similarly, adding to both sides of (5.16) the term

$$E_2=\left(1-\frac{\Delta t}{2}\right)\left(\epsilon_0\epsilon_\infty\|\mathscr{E}_y^n\|_{E_y}^2+\frac{\omega_0^2}{\epsilon_0\omega_p^2}\|\mathscr{P}^n\|_E^2+\frac{\|\mathscr{J}^n\|_E^2}{\epsilon_0\omega_p^2}\right)$$

and dividing the result by $1-\Delta t/2$, inequality (5.16) becomes

$$\begin{aligned}
&\mu_0\|\widetilde{\widetilde{H}}\|_H^2+\epsilon_0\epsilon_\infty\|\widetilde{\widetilde{E}}_x\|_{E_x}^2+\epsilon_0\epsilon_\infty\|\mathscr{E}_y^n\|_{E_y}^2+\frac{\omega_0^2}{\epsilon_0\omega_p^2}\|\mathscr{P}^n\|_E^2+\frac{\|\mathscr{J}^n\|_E^2}{\epsilon_0\omega_p^2}\\
&\le\frac{(1+\Delta t/2)}{(1-\Delta t/2)}\left[\mu_0\|\mathscr{H}^n\|_H^2+\epsilon_0\epsilon_\infty\|\|\mathscr{E}^n\|_E^2+\frac{\omega_0^2}{\epsilon_0\omega_p^2}\|\mathscr{P}^n\|_E^2+\frac{\|\mathscr{J}^n\|_E^2}{\epsilon_0\omega_p^2}\right]\\
&\quad+\frac{2\Delta t}{2-\Delta t}C_1(\Delta t^2+\Delta x^2+\Delta y^2)^2. \qquad (5.20)
\end{aligned}$$

Using (5.19) and the results obtained from (5.17) and (5.20) allows to eliminate the intermediate variables, so that

$$\begin{aligned}
&\frac{(1-\Delta t/2)}{(1+\Delta t/2)}\left[\mu_0\|\mathscr{H}^{n+1}\|_H^2+\epsilon_0\epsilon_\infty\|\mathscr{E}^{n+1}\|_E^2+\frac{\omega_0^2}{\epsilon_0\omega_p^2}\|\mathscr{P}^{n+1}\|_E^2+\frac{\|\mathscr{J}^{n+1}\|_E^2}{\epsilon_0\omega_p^2}\right]\\
&\le\frac{(1+\Delta t/2)^2}{(1-\Delta t/2)^2}\left[\mu_0\|\mathscr{H}^n\|_H^2+\epsilon_0\epsilon_\infty\|\mathscr{E}^n\|_E^2+\frac{\omega_0^2}{\epsilon_0\omega_p^2}\|\mathscr{P}^n\|_E^2+\frac{\|\mathscr{J}^n\|_E^2}{\epsilon_0\omega_p^2}\right]\\
&\quad+\frac{2C_4\Delta t(\Delta t^2+12)}{(2-\Delta t)^2(2+\Delta t)}(\Delta t^2+\Delta x^2+\Delta y^2)^2, \qquad (5.21)
\end{aligned}$$

where $C_4=\max\{C_1,C_2,C_3\}$. Since

$$\frac{1-\Delta t/2}{1+\Delta t/2}\ge 1-\Delta t,$$

the inequality (5.21) can be written in the form

$$(1-\Delta t)\mathbf{Err}_h^{n+1}\le\frac{(1+\Delta t/2)^2}{(1-\Delta t/2)^2}\mathbf{Err}_h^n+\frac{2C_4\Delta t(\Delta t^2+12)}{(2-\Delta t)^2(2+\Delta t)}(\Delta t^2+\Delta x^2+\Delta y^2)^2. \qquad (5.22)$$

If Δt is sufficiently small, we can simplify (5.22) as follows:

$$\mathbf{Err}_h^{n+1}\le e^{4\Delta t}\mathbf{Err}_h^n+\Delta tC_5(\Delta t^2+\Delta x^2+\Delta y^2)^2, \qquad (5.23)$$

where $C_5=5C_4$. Applying (5.23) recursively from time level n to 0 and using the fact that $N\Delta t=T$, we get

$$\mathbf{Err}_h^n\le e^{4T}\mathbf{Err}_h^0+C_6(\Delta t^2+\Delta x^2+\Delta y^2)^2,$$

where C_6 is a constant independent of $\Delta t,\Delta x$ and Δy. □

The convergence analysis of the SS-ML scheme can be proved similarly to the Theorem 5.1 as the following theorem.

Theorem 5.2. *Suppose that the exact solutions of electromagnetic fields are smooth enough:* $\mathbf{E},\mathbf{P},\mathbf{J}\in C^3(0,T;[C^3(\overline{\Omega})]^2)$ *and* $H\in C^3(0,T;C^3(\overline{\Omega}))$. *For all* $n\ge 0$, *let* $\mathbf{E}^n,\mathbf{P}^n,\mathbf{J}^n$, *and* H^n *be the solutions of the SS-ML scheme. Then for fixed* $T=N\Delta t>0$, *there exists a constant* C *independent of* $\Delta t,\Delta x$ *and* Δy *such that*

$$\max_{0\le n\le N}\mathbf{Err}_h^n\le e^{4T}\max_{0\le n\le N}\mathbf{Err}_h^0+C(\Delta t+\Delta x^2+\Delta y^2)^2.$$

6. Numerical Dispersion Analysis

In this section, we analyze the numerical dispersion of the splitting schemes by investigating the relationship between the wave number vector $\mathbf{k}$ and the angular frequency ω. To determine the dispersion relation for the splitting scheme, we suppose the discrete plane wave solutions of the Maxwell-Lorentz's equations are

$$U^{\gamma}_{\alpha,\beta} = U_0 e^{i(k_x \alpha \Delta x + k_y \beta \Delta y - \omega \gamma \Delta t)},$$

where $i = \sqrt{-1}$, the parameter U is one of the components of the electromagnetic field and k_x, k_y are components of the wave number vector $\mathbf{k}$ along the corresponding axis. We also define some notations $\zeta_x, \zeta_y, \zeta_t$ and Ψ_p as

$$\zeta_x = \frac{1}{\Delta x}\sin\left(\frac{k_x}{2}\Delta x\right), \quad \zeta_y = \frac{1}{\Delta y}\sin\left(\frac{k_y}{2}\Delta y\right), \quad \zeta_t = \frac{1}{\Delta t}\tan\left(\frac{\omega}{2}\Delta t\right),$$
$$\Psi_p = \tau\epsilon_s\omega_0^2 - 2i\epsilon_\infty\zeta_t - 4\epsilon_\infty\tau\zeta_t^2.$$

Consequently, the relationship between the wave number vectors and the angular frequency of the SS-ML scheme can be expressed as follows:

$$0 = \left(\tau\omega_p^2 - \Psi_p\right)\left[\Psi_p\left(\zeta_x^2 + \zeta_y^2\right) + \frac{\Delta t^2}{\epsilon_0\mu_0\epsilon_\infty}\left(\Psi_p - \tau\omega_p^2\left(1 + \Delta t^2\zeta_t^2\right)\right)\zeta_x^2\zeta_y^2\right]$$
$$+ \epsilon_0\mu_0\epsilon_\infty\Psi_p^2\zeta_t^2 + \Delta t^2\tau\omega_p^2\Psi_p\zeta_y^2\zeta_t^2. \tag{6.1}$$

Similarly, the wave number vectors and the angular frequency of the SM-ML scheme are related by

$$0 = \left(\tau\omega_p^2 - \Psi_p\right)\left[\Psi_p\left(\zeta_x^2 + \zeta_y^2\right) + \frac{\Delta t^2}{\epsilon_0\mu_0\epsilon_\infty}\left(\frac{\Psi_p}{2} - \tau\omega_p^2\left(1 + \Delta t^2\zeta_t^2\right) + \frac{\Delta t^2\Psi_p\zeta_y^2}{16\epsilon_0\mu_0\epsilon_\infty}\right)\zeta_x^2\zeta_y^2\right]$$
$$+ \left[\epsilon_0\mu_0\epsilon_\infty - \frac{\Delta t^4\zeta_y^2}{16\epsilon_0\mu_0\epsilon_\infty}\right]\Psi_p^2\zeta_t^2 + \Delta t^2\left[\tau\omega_p^2 - \frac{\Psi_p}{2}\right]\Psi_p\zeta_y^2\zeta_t^2. \tag{6.2}$$

The analytical dispersion relation for the Maxwell-Lorentz's equations is given by

$$k_{ex}^2 = \epsilon_0\mu_0\omega^2\,\frac{\epsilon_\infty\omega(i + \tau\omega) - \epsilon_s\tau\omega_0^2}{i\omega + \tau\omega^2 - \tau\omega_0^2}.$$

It is observed that the numerical dispersion relations (6.1) and (6.2) converge to this analytical relation as the mesh sizes and time steps approach zero.

7. Numerical Examples

We present numerical examples to support our theoretical findings in this section. We establish the spatial domain $\Omega = [0,1]\times[0,1]$ with perfect electric conditions,

$$E_x(x,0,t) = E_x(x,1,t) = E_y(0,y,t) = E_y(1,y,t) = 0 \quad \text{on} \quad t \in (0,T],$$

and assume a uniform mesh with $\Delta x = \Delta y = h$. We demonstrate our results by utilizing the analytical solution within the region Ω, which is enclosed by perfect electric boundary conditions

$$\begin{aligned}
H(x,y,t) &= \frac{|\mathbf{k}|^2}{\mu_0} e^{-\phi t} \cos(k_x \pi x) \cos(k_y \pi y), \\
E_x(x,y,t) &= -\frac{\phi}{\pi} k_y e^{-\phi t} \cos(k_x \pi x) \sin(k_y \pi y), \\
E_y(x,y,t) &= \frac{\phi}{\pi} k_x e^{-\phi t} \sin(k_x \pi x) \cos(k_y \pi y), \\
P_x(x,y,t) &= -\frac{k_y}{\pi} \alpha_l e^{-\phi t} \cos(k_x \pi x) \sin(k_y \pi y), \\
P_y(x,y,t) &= \frac{k_x}{\pi} \alpha_l e^{-\phi t} \sin(k_x \pi x) \cos(k_y \pi y), \\
J_x(x,y,t) &= -\frac{k_y}{\pi} \beta_l e^{-\phi t} \cos(k_x \pi x) \sin(k_y \pi y), \\
J_y(x,y,t) &= \frac{k_x}{\pi} \beta_l e^{-\phi t} \sin(k_x \pi x) \cos(k_y \pi y),
\end{aligned} \tag{7.1}$$

where $\mathbf{k} = (k_x, k_y)$ is a wave number vector and is assumed to be an integer vector, ϕ is a real number related by the equation

$$\phi^4 - \frac{\phi^3}{\tau} + \left(\omega_0^2 + \frac{\pi^2 |\mathbf{k}|^2}{\epsilon_0 \epsilon_\infty \mu_0} + \frac{\omega_p^2}{\epsilon_\infty} \right) \phi^2 - \frac{\pi^2 |\mathbf{k}|^2}{\mu_0 \epsilon_0 \epsilon_\infty \tau} \phi + \frac{\omega_0^2 \pi^2 |\mathbf{k}|^2}{\epsilon_0 \epsilon_\infty} = 0,$$

as well as α_l and β_l are functions relating to the wave number vector and ϕ as

$$\begin{aligned}
\beta_l(\phi, \mathbf{k}) &= \frac{1}{\mu_0} \left(\pi^2 |\mathbf{k}|^2 + \epsilon_0 \epsilon_\infty \mu_0 \phi^2 \right), \\
\alpha_l(\phi, \mathbf{k}) &= -\frac{\beta_l}{\phi} = \frac{1}{\omega_0^2 \tau} \left(\beta_l(-1 + \tau\phi) + \epsilon_0 \omega_p^2 \tau \phi \right).
\end{aligned}$$

Consequently, the exact energy of the analytic solution (7.1) over Ω is given by

$$\mathscr{E}(t) := \frac{|\mathbf{k}|}{2\pi} e^{-\phi t} \left[\epsilon_0 \epsilon_\infty \phi^2 + \frac{\pi^2 |\mathbf{k}|^2}{\mu_0} + \frac{\alpha_l^2 \omega_0^2}{\epsilon_0 \omega_p^2} + \frac{\beta_l^2}{\epsilon_0 \omega_p^2} \right]^{1/2}.$$

If not specified otherwise, the parameters will be set to $T = 1, \mu_0 = 1, \epsilon_0 = 1, \epsilon_\infty = 1, \omega_0 = 1, \tau = 0.4, \epsilon_s = 2, \epsilon_q = 2$, $k_x = 1$ and $k_y = -2$.

7.1. Validation of energy decay property

In this section, we demonstrate the energy decay of our schemes by computing the maximum difference in discrete energy between two consecutive time steps, denoted as $\max_{0 \le n \le N} (\mathscr{E}_L^{n+1} - \mathscr{E}_L^n)$. By choosing a time step size of $\Delta t = 0.02$ with different CFL numbers, it can be observed from Table 1 that the discrete energy difference remains negative for both the SS-ML and SM-ML schemes. The results confirm the energy decay property stated in Theorems 4.1 and 4.2.

Table 1: The comparison of differences between two time steps of the discrete energy for various values of CFL numbers.

N	$\nu=0.2$		$\nu=0.5$		$\nu=1$	
	SS-ML	SM-ML	SS-ML	SM-ML	SS-ML	SM-ML
50	-2.4025	-2.4048	-6.0011	-6.0052	-12.0006	-12.0083
100	-2.3954	-2.3961	-5.9869	-5.9885	-11.9733	-11.9766
200	-2.3921	-2.3924	-5.9799	-5.9806	-11.9596	-11.9611
400	-2.3906	-2.3907	-5.9764	-5.9768	-11.9528	-11.9535

7.2. The convergence rate of numerical solutions

Suppose that $H(t^n), \mathbf{E}(t^n), \mathbf{P}(t^n), \mathbf{J}(t^n)$ and $H^n, \mathbf{E}^n, \mathbf{P}^n, \mathbf{J}^n$ are the exact and numerical solutions at time t^n, respectively. The absolute error Err_h of the numerical solution obtained by the splitting schemes is defined by

$$\mathrm{Err}_h := \max_{0\le n\le N} \sqrt{\mu_0 \mathscr{E}_H(t^n) + \epsilon_0\epsilon_\infty \mathscr{E}_E(t^n) + \frac{\omega_0^2}{\epsilon_0\omega_p^2}\mathscr{E}_P(t^n) + \frac{1}{\epsilon_0\omega_p^2}\mathscr{E}_J(t^n)}, \tag{7.2}$$

where

$$\mathscr{E}_H(t^n) = \|H(t^n) - H^n\|_H^2, \quad \mathscr{E}_E(t^n) = \|\mathbf{E}(t^n) - \mathbf{E}^n\|_E^2,$$
$$\mathscr{E}_P(t^n) = \|\mathbf{P}(t^n) - \mathbf{P}^n\|_E^2, \quad \mathscr{E}_J(t^n) = \|\mathbf{J}(t^n) - \mathbf{J}^n\|_E^2.$$

In this section, we present the convergence analysis of the 2D Maxwell-Lorentz equations using the SS-ML and SM-ML schemes. We explore various CFL number values, specifically $\nu = 0.2, 0.5, 1$. The simulations employ a time step size of $\Delta t = 0.02$, and we conduct additional simulations with halved time step sizes, resulting in a total of five simulations.

Tables 2-4 and Fig. 2 show the error and convergence rates for SS-ML, SM-ML, and Yee schemes. It is observed that for small CFL numbers, the error of the Yee scheme is comparable to the SM-ML scheme but smaller than the SS-ML scheme. Moreover, the SS-ML scheme exhibits first-order accuracy, whereas both the SM-ML scheme and Yee scheme achieve second-order accuracy. However, despite its lower error, the Yee scheme is limited by the CFL requirement [2, 5, 24]. These experimental results validate the findings

Table 2: The comparison of errors and convergence rates of different schemes where $\nu = 0.2$.

Case $\nu=0.2$		Numbers of time steps N				
Scheme		50	100	200	400	800
SS-ML	Err_h	2.574e-01	1.267e-01	6.329e-02	3.168e-02	1.586e-02
	Rate		1.022	1.002	0.998	0.999
SM-ML	Err_h	7.502e-02	1.865e-02	4.656e-03	1.164e-03	2.909e-04
	Rate		2.008	2.002	2.001	2.000
Yee	Err_h	7.208e-02	1.788e-02	4.459e-03	1.114e-03	2.784e-04
	Rate		2.012	2.003	2.001	2.000

Table 3: The comparison of errors and convergence rates of different schemes where $\nu = 0.5$.

Case $\nu = 0.5$		Numbers of time steps N				
Scheme		50	100	200	400	800
SS-ML	Err_h	2.534e-01	1.269e-02	6.347e-02	3.174e-02	1.587e-02
	Rate		0.998	0.999	1.000	1.000
SM-ML	Err_h	1.549e-02	3.874e-03	9.684e-04	2.421e-04	6.053e-05
	Rate		1.999	2.000	2.000	2.000
Yee	Err_h	1.149e-02	2.868e-03	7.166e-04	1.791e-04	4.476e-05
	Rate		2.003	2.001	2.001	2.000

Table 4: The comparison of errors and convergence rates of different schemes where $\nu = 1$.

Case $\nu = 1$		Numbers of time steps N				
Scheme		50	100	200	400	800
SS-ML	Err_h	2.540e-01	1.270e-01	6.351e-02	3.175e-02	1.588e-02
	Rate		1.000	1.000	1.000	1.000
SM-ML	Err_h	7.916e-03	1.981e-03	4.953e-04	1.238e-04	3.096e-05
	Rate		1.999	2.000	2.000	2.000

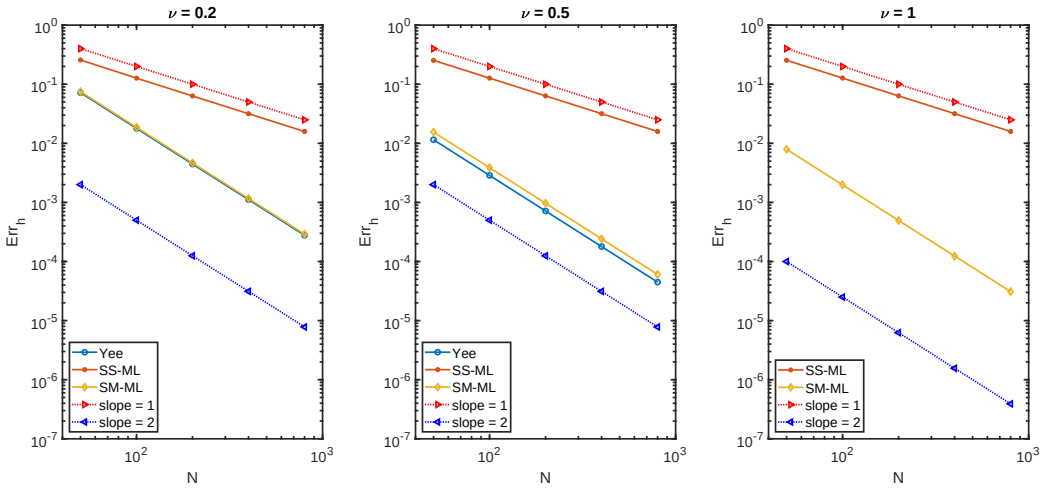

Figure 2: The comparison of errors and convergence rates for various values of CFL numbers: Left: $\nu = 0.2$, Middle: $\nu = 0.5$, Right: $\nu = 1$.

presented in Theorems 5.1 and 5.2 regarding the convergence of the SM-ML and SS-ML schemes.

In the first two figures of Fig. 3, we compare the error (7.2) of all schemes over the long time computation by setting $T = 200$ and $\Delta t = 0.02$. For CFL numbers $\nu = 0.2$ and $\nu = 0.5$, the error of each scheme is plotted against the time level n. The error shows fluctuations for smaller time steps but stabilizes as the time steps increase. The zoom plot reflects the error relative to the case when $T = 1$, consistent with the results in Tables 2 and 3. This indicates

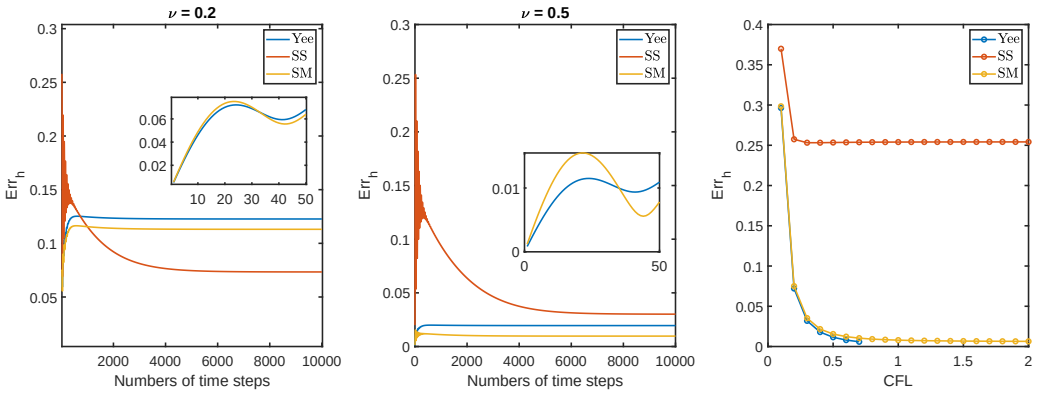

Figure 3: The comparison of relative error in energy: Left: versus to numbers of time steps, Right: versus to CFL numbers.

that both the splitting schemes and the Yee scheme exhibit stability under CFL conditions, regardless of the number of time steps. However, in order to address the limitations of the CFL conditions, we examine the maximum stable CFL numbers for the splitting schemes in comparison to the Yee scheme. Specifically, we focus on CFL numbers $0 < \nu \leq 2$ with $\Delta t = 0.02$ and $T = 1$. In the right figure of Fig. 3, the errors of the splitting schemes decrease as the CFL numbers increase, while the error of the Yee scheme is overestimated for CFL numbers higher than the theoretical analysis suggests [2, 24, 26].

7.3. Dispersion relations

We analyze the numerical dispersion of the splitting schemes and compare them with the Yee scheme in this section. The wave number vector $\mathbf{k} = (k_x, k_y)$ can be represented in polar coordinates as $k_x = k\cos(\theta)$ and $k_y = k\sin(\theta)$, where θ is the propagation angle and k is the scalar wavenumber. In order to compare the analytic dispersion relation (6.1) with the corresponding numerical dispersion relations (6.1) and (6.2), we introduce the numerical phase error, denoted Φ as

$$\Phi = \left| \frac{k_{ex} - k_{num}}{k_{ex}} \right|,$$

where k_{ex} and k_{num} are the scalar wavenumber of the analytic and numerical (SS-ML and SM-ML schemes) dispersion relations, respectively.

In Fig. 4, the polar plots depict the phase error and propagation angle for different CFL numbers. These factors are essential for accurately predicting electromagnetic wave behavior and designing various electromagnetic systems. The plots show the phase error for different propagation angles θ and CFL numbers $\nu = 0.1, 0.2, 0.5$, with fixed values of angular frequency $\omega = 1$ and time step size $\Delta t = 0.02$. The phase error of the splitting schemes and the Yee scheme varies with θ and ν, allowing for larger time steps. Among the schemes, the SS-ML scheme consistently exhibits the highest error, while the Yee scheme

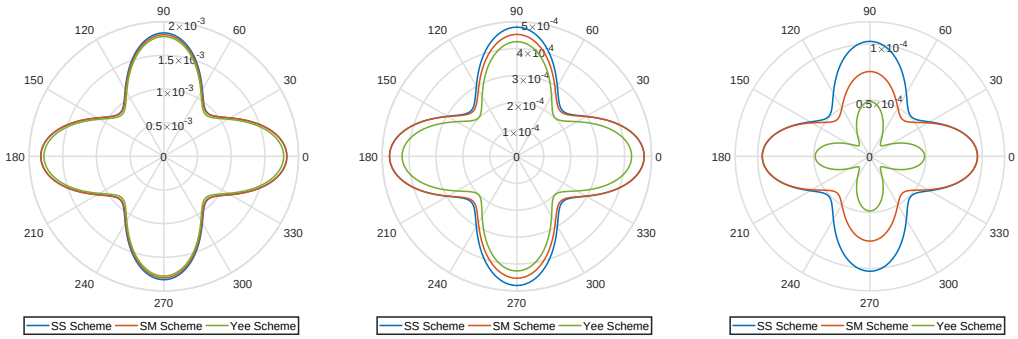

Figure 4: The comparison of the numerical phase errors between the analytic and numerical dispersion relation for various values of CFL numbers. Left: $\nu = 0.1$. Middle: $\nu = 0.2$. Right: $\nu = 0.5$.

has the lowest dispersion error. At angles of $(2n+1)\pi/4$, where n is an integer, all three schemes exhibit minimal phase errors. Depending on the chosen angle, the phase errors of the schemes are comparable to those of the first-order SS-ML scheme and the second-order SM-ML and Yee schemes in terms of time accuracy.

7.4. Characteristic behavior of phase error over frequency ranges

In this section, we examine relative phase error in wave numbers across high and low resonance frequency ranges. The frequency domain of interest, $\omega/\omega_0 \in (0,2)$, spans both low and high frequencies. Drawing from $[1,5]$, we define key parameters: $\epsilon_0 = 1$, $\epsilon_s = 2.25$, $\tau = 1.7857 \times 10^{-16} s^{-1}$, and $\omega_0 = 4 \times 10^{16}$ rad/s. These values are standard in physical optics research and are indicative of a medium with high absorption and dispersion properties. The selection of time steps will be influenced by the temporal refinement factor, $h_0 = \omega_0 \Delta t$.

Fig. 5 depicts phase errors associated with each scheme as a function of angular frequency ω, which impacts wave propagation accuracy and electromagnetic field behavior. We generate these plots with h_0 set to 0.01 and the angle at $\pi/4$ for various CFL numbers. The phase error for all three methods consistently exhibits the same directional pattern, alternating between higher and lower values across different frequency ranges. Notably, the Yee method consistently demonstrates lower phase errors than the other two methods within the frequency intervals of $0-\omega_0$ and $1.5\omega_0 - 2\omega_0$. Furthermore, it is evident that as the CFL number increases, the phase error decreases.

To compare the performance of the proposed splitting methods against the Yee scheme, we examine the relative error in wavenumber over the low-to-high-frequency range. Here, the phase error is analyzed by varying the propagation angles and frequencies of interest within the range $\omega/\omega_0 \in (0,2)$. Fig. 6 presents a polar plot of the logarithmic phase error, where the surfaces represent the error for different normalized frequencies. The simulations are conducted with a temporal refinement factor of $h_0 = 0.001$ and varying CFL values of $\nu = 0.1, 0.2, 0.5$. It is apparent that the phase error for all three methods displays a pattern of alternating between low and high values across different frequency ranges and CFL values. As the CFL value increases, the phase error consistently decreases

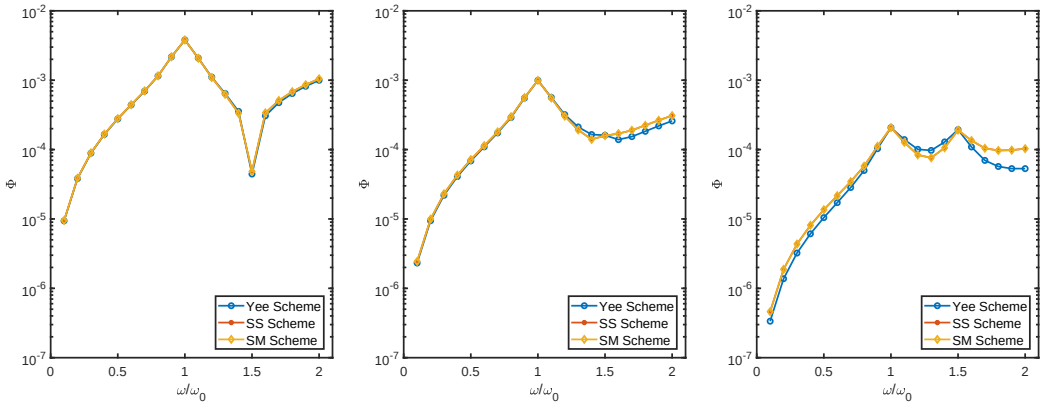

Figure 5: Comparison of numerical phase errors in the frequency domain for different CFL numbers. Left: $\nu = 0.1$. Middle: $\nu = 0.2$. Right: $\nu = 0.5$.

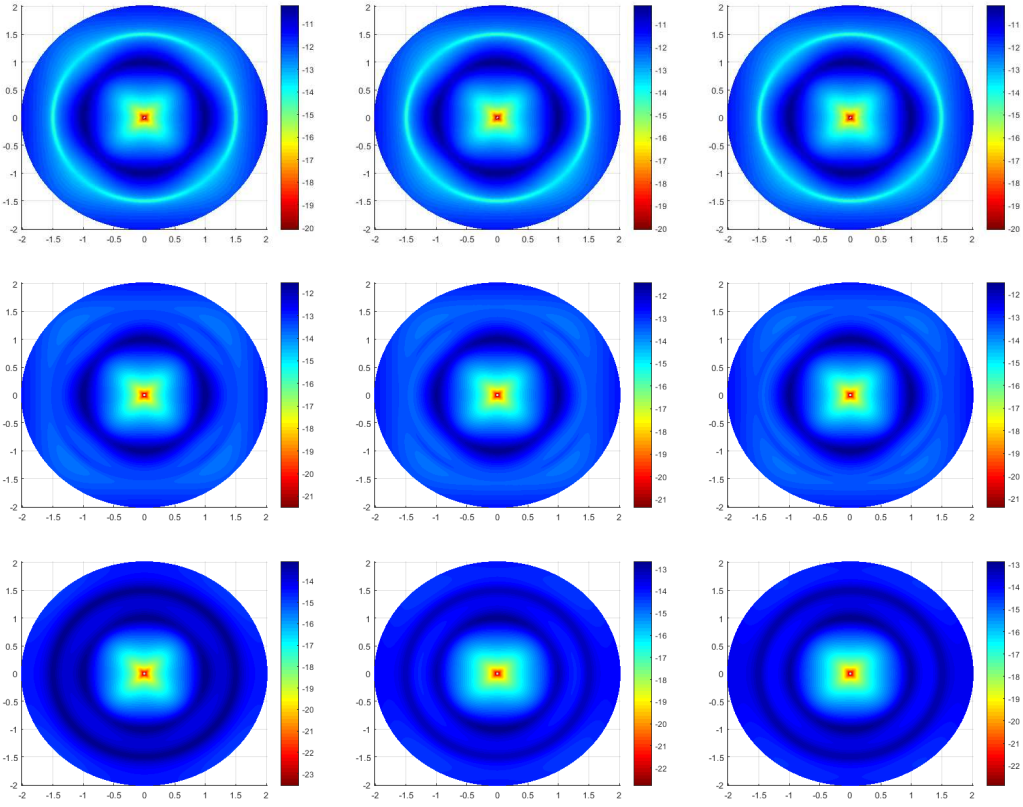

Figure 6: Comparison of numerical phase errors in the frequency domain for different CFL numbers. First Column: Yee Scheme, Second Column: SS-Scheme, Third Column: SM-Scheme. First Row: $\nu = 0.1$. Second Row: $\nu = 0.2$. Third Row: $\nu = 0.5$.

for each examined method. Furthermore, the propagation angle also influences the phase error. It is evident that, regardless of the values of h_0 and CFL, all methods yield the lowest phase error when the propagation angle is $(2n+1)\pi/4$, where n is an integer. These observations highlight that the proposed methods, SS-ML and SM-ML, accurately capture wave behavior at both low and high frequencies, yielding results comparable to the Yee scheme while operating without the constraints of CFL conditions.

8. Conclusions

The results of this study contribute to the development and analysis of efficient numerical methods for solving Maxwell's equations in Lorentz dispersive media. The proposed splitting schemes, the sequential scheme and the Strang-Marchuk splitting scheme, have effectively achieved unconditional stability in numerical simulations. Rigorous stability and convergence analyses demonstrate that these methods maintain the energy decay properties of the continuous model. The accuracy and performance of the schemes in capturing wave propagation behavior are further validated through numerical dispersion analysis. Empirical evidence from numerical simulations supports the theoretical findings and confirms the validity of the proposed methods. Future research can explore extending these methods to higher dimensions or more complex scenarios.

Acknowledgments

The author is grateful to the anonymous referees for their many helpful comments and suggestions which greatly improved the quality of this paper.

References

[1] H.T. Banks, V.A. Bokil and N.L. Gibson, *Analysis of stability and dispersion in a finite element method for Debye and Lorentz dispersive media*, Numer. Methods Partial Differential Equations **25**, 885–917 (2009).

[2] B. Bidégaray-Fesquet, *Stability of FD-TD schemes for Maxwell-Debye and Maxwell-Lorentz equations*, SIAM J. Numer. Anal. **46**, 2551–2566 (2008).

[3] C.F. Bohren and D.R. Huffman, *Absorption and Scattering of Light by Small Particles*, John Wiley & Sons (2008).

[4] V.A. Bokil, Y. Cheng, Y. Jiang, F. Li and P. Sakkaplangkul, *High spatial order energy stable FDTD methods for Maxwell's equations in nonlinear optical media in one dimension*, J. Sci. Comput. **77**, 330–371 (2018).

[5] V.A. Bokil and N.L. Gibson, *Analysis of spatial high-order finite difference methods for Maxwell's equations in dispersive media*, IMA J. Numer. Anal. **32**, 926–956 (2012).

[6] V.A. Bokil, O.A. Keefer and A.Y. Leung, *Operator splitting methods for Maxwell's equations in dispersive media with orientational polarization*, J. Comput. Appl. Math. **263**, 160–188 (2014).

[7] M.A. Botchev, I. Faragó and R. Horváth, *Application of operator splitting to the Maxwell equations including a source term*, Appl. Numer. Math. **59**, 522–541 (2009).

[8] W. Chen, X. Li and D. Liang, *Energy-conserved splitting FDTD methods for Maxwell's equations*, Numer. Math. **108**, 445–485 (2008).

[9] W. Chen, X. Li and D. Liang, *Energy-conserved splitting finite-difference time-domain methods for Maxwell's equations in three dimensions*, SIAM J. Numer. Anal. **48**, 1530–1554 (2010).
[10] C.M. Furse, J.Y. Chen and O.P. Gandhi, *The use of the frequency-dependent finite-difference time-domain method for induced current and SAR calculations for a heterogeneous model of the human body*, IEEE Trans. Electromagn. Compat. **36**, 128–133 (1994).
[11] A. Gansen, M. El Hachemi, S. Belouettar, O. Hassan and K. Morgan, *A 3D unstructured mesh FDTD scheme for EM modelling*, Arch. Comput. Methods Eng. **28**, 181–213 (2021).
[12] L. Gao, X. Sang and R. Shi, *Energy identities and stability analysis of the Yee scheme for 3D Maxwell equations*, J.Comput. Appl. Math. **13**, 788–813 (2020).
[13] S.G. Garcia, T.W. Lee and S.C. Hagness, *On the accuracy of the ADI-FDTD method*, IEEE Antennas Wireless Propag. **1**, 31–34 (2002).
[14] J. Hong, L. Ji and L. Kong, *Energy-dissipation splitting finite-difference time-domain method for Maxwell equations with perfectly matched layers*, J. Comput. Phys **269**, 201–214 (2014).
[15] T. Kashiwa and I. Fukai, *A treatment by the FD-TD method of the dispersive characteristics associated with electronic polarization*, Microw. Opt. Technol. Lett. **3**, 203–205 (1990).
[16] K. Kormann and E. Sonnendrücker, *Energy-conserving time propagation for a structure-preserving particle-in-cell Vlasov-Maxwell solver*, J. Comput. Phys. **425**, 109890 (2021).
[17] S. Lanteri and C. Scheid, *Convergence of a discontinuous Galerkin scheme for the mixed time-domain Maxwell's equations in dispersive media*, IMA J. Numer. Anal. **33**, 432–459 (2013).
[18] J. Lee and B. Fornberg, *A split step approach for the 3-D Maxwell's equations*, J. Comput. Appl. Math. **158**, 485–505 (2003).
[19] J. Li, *Unified analysis of leap-frog methods for solving time-domain Maxwell's equations in dispersive media*, J. Sci. Comput. **47**, 1–26 (2011).
[20] J. Li and S. Shields, *Superconvergence analysis of Yee scheme for metamaterial Maxwell's equations on non-uniform rectangular meshes*, Numer. Math. **134**, 741–781 (2016).
[21] P. Monk and E. Süli, *A convergence analysis of Yee's scheme on nonuniform grids*, SIAM J. Numer. Anal. **31**, 393–412 (1994).
[22] P. Monk and E. Süli, *Error estimates for Yee's method on non-uniform grids*, IEEE Trans. Magn. **30**, 3200–3203 (1994).
[23] L. Novotny and B. Hecht, *Principles of Nano-Optics*, Cambridge University Press (2012).
[24] P.G. Petropoulos, *Stability and phase error analysis of FD-TD in dispersive dielectrics*, IEEE Trans. Antennas Propag. **42**, 62–69 (1994).
[25] P. Sakkaplangkul, *Convergence analysis of operator splitting methods for Maxwell's equations in dispersive media of Debye type*, J. Appl. Math. Comput. **69**, 4587–4616 (2023).
[26] P. Sakkaplangkul and V.A. Bokil, *Convergence analysis of Yee-FDTD schemes for 3D Maxwell's equations in linear dispersive media*, Int. J. Numer. Anal. Model. **18**, 524–568 (2021).
[27] D.R. Smith and D. Schurig, *Electromagnetic wave propagation in media with indefinite permittivity and permeability tensors*, Phys. Rev. Lett. **90**, 077405 (2003).
[28] A. Taflove, S.C. Hagness M. Piket-May, *Computational Electromagnetics: The Finite-Difference Time-Domain Method*, in: *The Electrical Engineering Handbook*, Elsevier Inc. 629–670 (2005).
[29] K. Yee, *Numerical solution of initial boundary value problems involving Maxwell's equations in isotropic media*, IEEE Trans. Antennas Propag. **14**, 302–307 (1966).
[30] J.L. Young and R.O. Nelson, *A summary and systematic analysis of FDTD algorithms for linearly dispersive media*, IEEE Antennas Propag. Mag. **4**, 61–126 (2001).